UNIVERSITY OF MANITOBA

MECH 4860 – Engineering Design

Geoclimatic Energy Project

Final Report

Project Sponsor: Joe Matula (Roofequip Welding Ltd)
Course Instructor: Dr. P. Labossiere
Project Advisor: Dr. D. Kuhn

Team Number 12

Team Members

Osaghae Irianan _____
Graham Leverick _____
Shawn Stargardter _____
JaeHo Choi _____

Submission Date: December 6th, 2010

Team Geoclimatic (Team #12)
E1-451 EITC
University of Manitoba
Winnipeg, MB
R3T 5V6

December 6, 2010

Dr. Paul E. Labossiere
E1-546 EITC
University of Manitoba
Winnipeg, MB
R3T 5V6

Dear Dr. Labossiere,

Please find the enclosed report entitled *Geoclimatic Energy Project: Final Report* submitted this 6th day of December 2010.

The concept of Geoclimatic energy comes from the mind of entrepreneur Joe Matula. Geoclimatic energy is intended as an improvement to conventional geothermal heat pumps by not only providing a home's heating and cooling requirements, but to also generate surplus electricity from seasonal temperature variations.

The enclosed draft report begins by introducing the concept of Geoclimatic energy and the design specifications and requirements provided to the team by Mr. Matula. The results from the conceptual design phase of the project are then summarized. The report then contains a detailed analysis of the thermal energy cycle performed by Mr. Leverick. The report continues with an analysis of thermal energy storage performed by Mr. Stargardter, an examination of environmental and regulatory considerations by Mr. Choi and an economic analysis which was performed by Mr. Irianan. The report concludes with a summary of our findings and our recommendations. This report draws the conclusion that although there are promising aspects to the concept of Geoclimatic energy, there are also a number of major issues which must be overcome before it can become a viable source of heat and energy.

Please feel free to contact Mr. Graham Leverick by phone or by e-mail at Graham_Leverick@umanitoba.ca if you have any questions or concerns.

Kind Regards,

O. Irianan

G. Leverick

S. Stargardter

J. Cho

Table of Contents

List of Figures

List of Tables

Glossary of Terms

Adiabatic – a process which occurs without heat loss

Enthalpy – a thermodynamic property which measures the total energy of a thermodynamic system [1]

Isobaric –a process which occurs at constant pressure

Isentropic – a process which occurs at constant entropy or adiabatically

Porosity – a property relating the volume of voids in a material to the total volume

Permeability – a property expressing the potential flow rate of water within an aquifer.

I. Executive Summary

The concept of Geoclimatic energy is intended as an improvement to conventional geothermal heat pumps by not only providing a home's heating and cooling requirements, but to also generate surplus electricity from seasonal temperature variations. A modified heat pump cycle has been designed which can serve the function of a geothermal heat pump, while simultaneously generating a small surplus of electricity of approximately 2 kW. The modified heat pump cycle can take the place of a conventional geothermal heat pump, and can deliver approximately 30 kW of space heating, 130 kW of water heating and 13 kW of air conditioning capacity. The designed cycle has an efficiency of 154% in the summer and 519% in the winter. A cornerstone to this modified heat pump cycle is utilizing an aquifer thermal storage system.

It has been demonstrated that the aquifer thermal storage system will be effective at storing thermal energy for long periods of time and with small thermal losses. With the two wells set to a spacing of 50 (m), there is an increase in temperature at the other well of only 0.89 ℃, which was deemed to be an acceptable temperature increase. It was also shown that the temperature in the water stored in the hot well would fall by not more than 10 ℃ of the course of a six month storage period, suggesting a thermal storage efficiency of 83.33%.

II. Introduction

The objective of this project is to design a system to collect and store thermal energy from the ambient environment and to use that energy to meet the thermal and electrical energy needs of a household. This system shares similarities with conventional geothermal heat pumps used to heat and cool some homes in Manitoba. The system is designed in two components; the heat pump and power cycle and the thermal energy storage system.

The center-point of the design is a modified heat pump cycle, which not only serves as a heat pump, but also produces net power to generate electricity. This cycle will operate based on the temperature difference between stored thermal energy and ambient conditions. As a result, the system will function differently depending on the season. Thermal energy is to be stored in the aquifer beneath the city of Winnipeg. Two wells will be drilled down into the aquifer; one well will act as a “hot well”, while the other will act as a “cold well”. This system will collect thermal energy during the summer months, store that energy in the “hot well”, and draw upon that energy in the winter time to provide heat. Furthermore, cold water will be collected during the winter time in order to meet the cooling demand of the home during the summer.

This project is motivated by the growing demand for alternative sources of energy, as issues such as the trend of increasing energy consumption, the prospect of peak oil, and global warming become more urgent. Many alternative energy sources are already being harnessed, including wind, solar and hydro power. One possible source of energy that is yet to be investigated is the drastic temperature difference that is experienced in certain extreme continental climates, such as Winnipeg. Entrepreneur Joe Matula has developed a concept, tentatively coined “Geoclimatic Energy”, which has the potential to harness power from our extreme seasons. If successful, this system has the potential to reduce or eliminate the dependence of a household on electrical power and fossil fuels for heating.

III. Customer Specifications

Based on data and specifications provided by our client, and the information provided in the project background, the client`s needs were interpreted and are summarized TABLE I.

TABLE I: THE NEEDS EXPRESSED BY THE CLIENT

NEED	Imp
Use Dual Wells to Store Cold and Hot Water	5
Secure the Necessary Flow Rate of Water to and From the Wells	3
Exchange Heat Efficiently Between Water and Working Fluid	4
Generate Net Power	4
The System Should Function in All Seasons	4
Maintain Constant Reservoir (Water Table) Volume	3
No Environmental Contamination by the Working Fluid	2
Minimize Ecological Impact of the System	2
Optimize Resources as Well as Reduce Cost of the System	3
Ease of Operation and Maintenance	1

The client's needs are presented on a scale of importance from one to five, where one represents a non-essential desire and five represents a critical aspect in the system design. It should be noted that this was very much a conceptual study initially, and that many of these parameters could not be quantified with the data which was available at the time. TABLE I also describes some of the system constraints imposed on the system, such as minimizing the environmental impact of the system. Additional constraints and specifications were determined later as the analysis proceeded and more information became available.

IV. Design Overview

The designed Geoclimatic energy system functions similarly to a conventional geothermal heat pump. The heat pump in integrated with the home's HVAC system to provide air conditioning in the summer, and water and air heating in the winter. The electrical generator is integrated with the house's electrical system to supplement grid electricity. During peak generating times, excess power is used to "reverse the meter" by providing power to the grid. Figure 1 provides a visual overview of a Geoclimatic energy system.

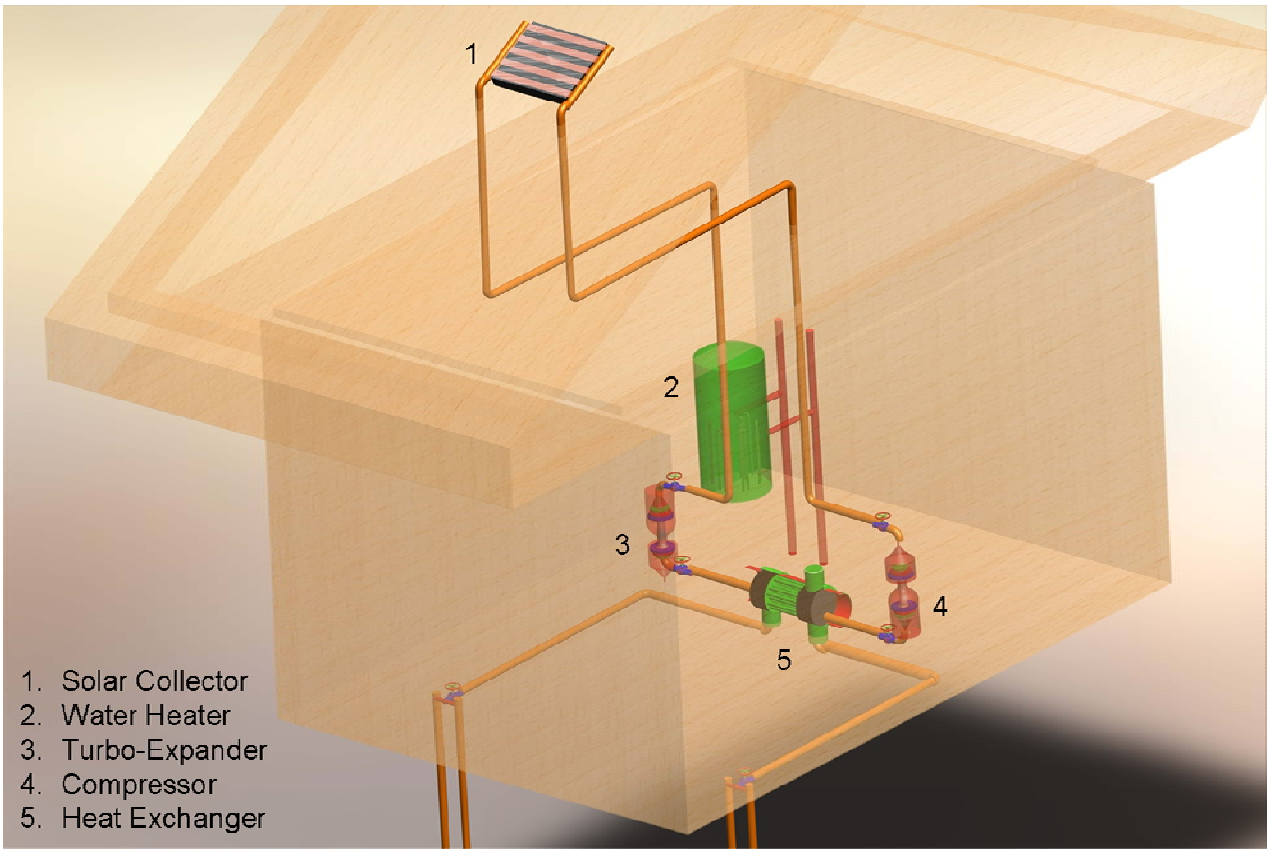

Figure 1 - Overview of a Geoclimatic Energy System

Two 20cm diameter wells, spaced 50m apart are drilled 120 m into the ground. Two 8 cm diameter PVC pipes are inserted into each well; one to draw water, and one to remove water. The draw pipe is equipped with a DC well pump and a screen filter to remove particle impurities from the water drawn from the aquifer. In the summer, water is drawn from the cold well,

heated, and returned to the hot well. In the winter, water is drawn from the hot well, cooled and stored in the cold well.

The water drawn from the wells exchanges heat with an R134a modified heat pump cycle. Figure 2 shows the heat and power flow through this modified heat pump cycle.

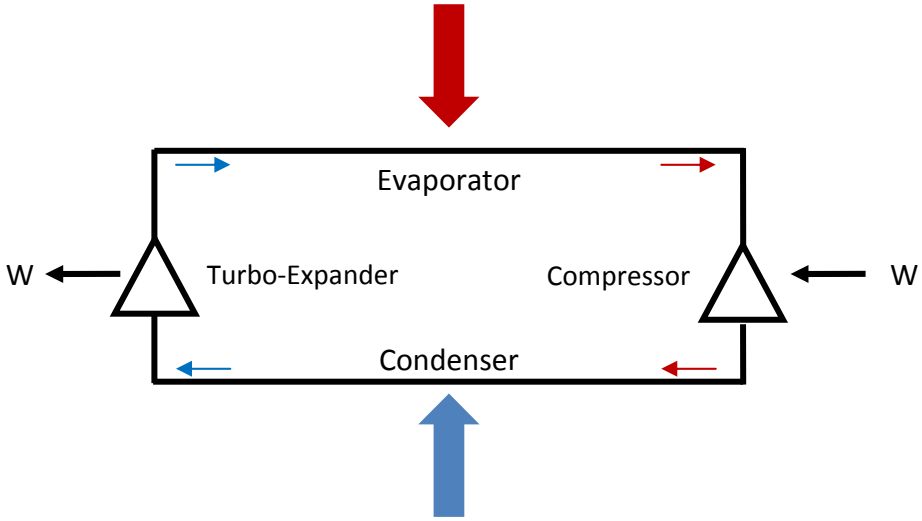

Figure 2 - Modified Heat Pump Cycle

In the summer, the water drawn from the cold well is used to cool the R134a in the condenser. The R134a is evaporated in the summer by functioning as an air conditioner to cool the house and by passing through the solar collector. In the winter, the water drawn from the hot well is used to heat the R134a in the evaporator. The R134a is condensed in the winter by heating the home's air and water. Power is extracted from the modified heat pump cycle using a turbo-expander. The power generated by the turbo-expander is used to power the compressor and well pump. Any excess electricity is used to provide electricity to the house and the grid.

V. Thermal Energy Cycle

A. Introduction to the Thermal Energy Cycle

The thermal energy cycle is the process through which power is generated from the temperature difference between the water drawn from the aquifer and the ambient

temperature. This process involves phase transformations of the working fluid. In our design, we selected R134a as the working fluid due to its desirable properties in the operating temperature range, as well as its low toxicity and non-flammable nature.

Two different cycles are investigated in this study; a modified heat pump cycle and a Rankine cycle. The proposed design utilizes the modified heat pump cycle. A discussion of the Rankine cycle is included to address its shortfalls for use in Geoclimatic Energy.

A typical heat pump cycle operates similar to a refrigerator by transferring heat from a low temperature sink to a high temperature sink by inputting energy in the form of a compressor. A Pressure-Enthalpy diagram of a typical heat pump cycle is shown in Figure 3. A Pressure-Enthalpy diagram shows the working fluid's transformation of enthalpy and pressure throughout each process in the cycle.

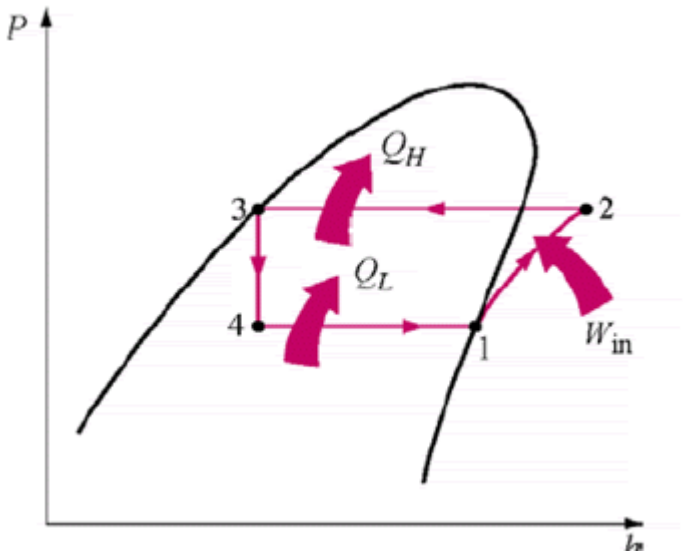

1-2: Compressor

2-3: Condenser

3-4: Expansion Valve

4-1: Evaporator

Figure 3 - Pressure-Enthalpy Diagram of a Typical Heat Pump/Refrigeration Cycle [2]

From 1-2, the fluid undergoes isentropic compression, requiring an input of work, W_{in}. From 2-3, the fluid isobarically transfers heat to the high temperature source. The fluid is then expanded through a valve from 3-4, and absorb heats from the low temperature sink isobarically from 1-4.

We have modified the typical heat pump cycle in order to generate power by absorbing heat from the high temperature sink and dissipating it to the low temperature sink. The ideal modified heat pump cycle is shown in Figure 4.

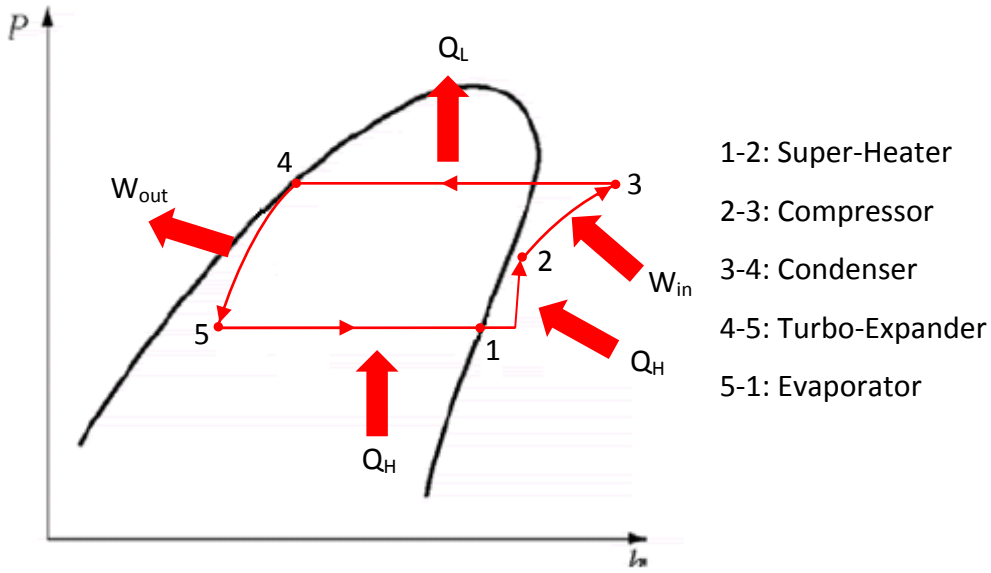

Figure 4 - Pressure-Enthalpy Diagram of the Ideal Modified Heat Pump Cycle

In the ideal case of our modified heat pump cycle, the fluid first undergoes a super-heating process from 1-2. This super-heating process starts with isobaric heating of the fluid while it simultaneously passes through an expander. The fluid is then isothermally compressed by constricting the flow through a nozzle and dissipating heat. A mechanical compressor than isentropically compresses the fluid from 2-3. The fluid then transfers heat to the low temperature source isobarically from 3-4. From 4-5 power is extracted through isentropic expansion in a turbo-expander. Finally, heat is absorbed from the high temperature source from 5-1.

The Rankine cycle also extracts power by absorbing heat from the high temperature sink and dissipating it to the low temperature sink. An ideal Rankine cycle is shown in Figure 5.

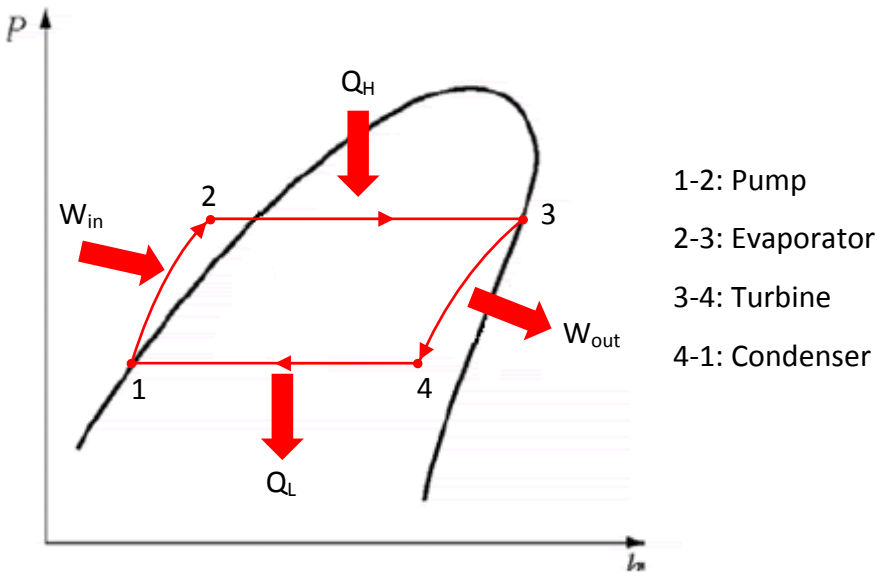

Figure 5 - Pressure-Enthalpy Diagram of an Ideal Rankine Cycle

From 1-2, the working fluid is pressurized isentropically by a pump. The fluid is then heated by the high temperature heat sink from 2-3. From 3-4, the working fluid is expanded through a turbine to generate power, W_{out}. The fluid is finally condensed by the low temperature sink from 4-1.

The primary difference between the Rankine cycle and the modified heat pump cycle is that the Rankine cycle extracts power in the vapour phase, whereas the modified heat pump cycle extracts power from a liquid phase to a mixed state. Another key difference is that a Rankine cycle is evaporated at a high temperature and condensed at cool temperature, whereas the modified heat pump cycle is evaporated at a low temperature and condensed at a high temperature. This means that the temperature range of the fluid in the modified heat pump cycle can be larger than that of a Rankine cycle operating between the same two heat sinks. This difference is of vital importance to the designed system because the heat sinks in a Geoclimatic Energy system have a very small temperature difference.

B. Seasonal Cycles

Since the cycles operate differently in the winter and summer, the following subsections describe the operation of a modified heat pump cycle and Rankine cycle in those seasons.

1. Modified Heat Pump Cycle

Figure 6 shows the operation of the modified heat pump cycle in the summer. The five states from the pressure-enthalpy diagram in Figure 4 have been labelled to aid understanding of the process.

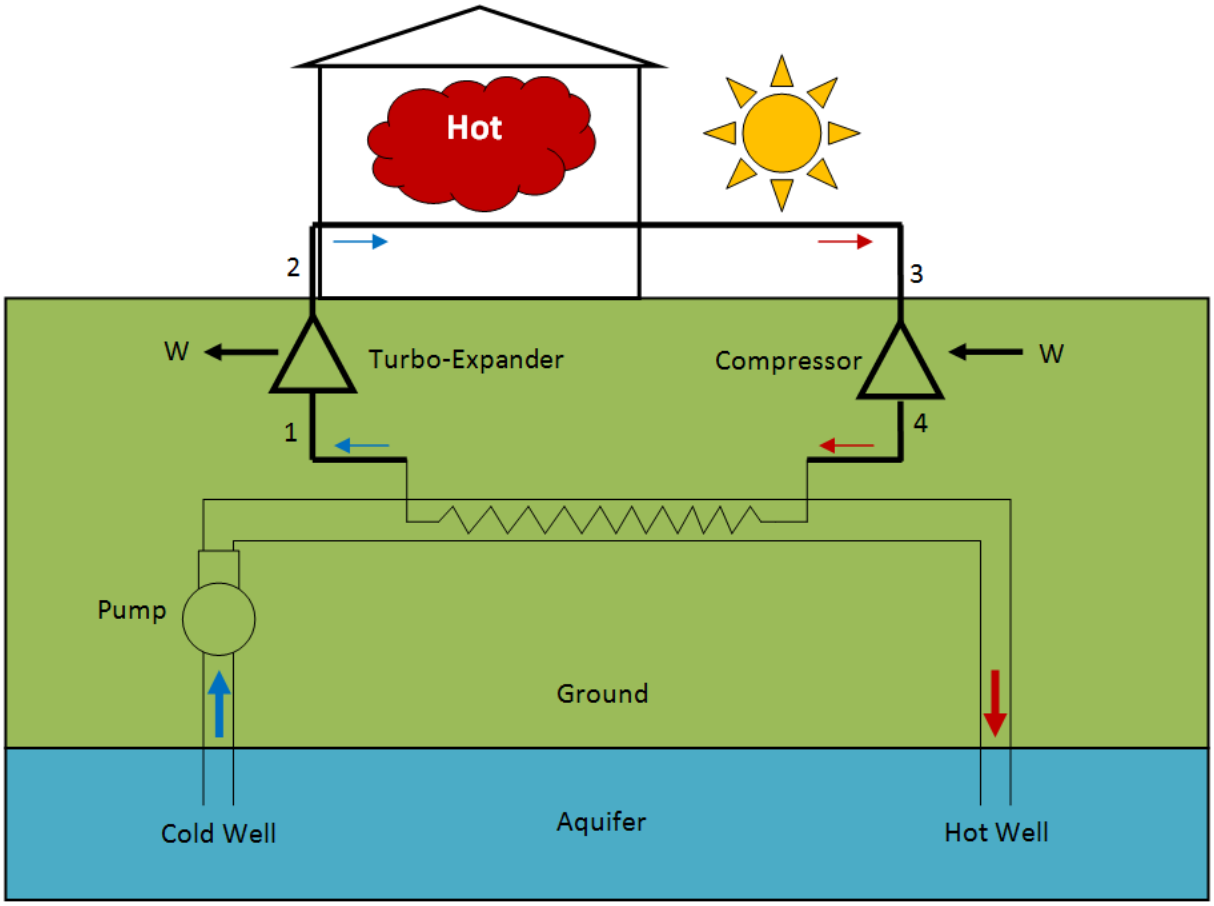

Figure 6 - Modified Heat Pump Cycle Operation in the Summer

The cold mixed-phase R134a which exits the turbo-expander at state 5 is first used to provide air conditioning in the home. As the fluid is heated, it becomes a saturated vapour, at state 1. The fluid is then super-heated using a solar collector to reach state 2. Next, the R134a is compressed mechanically using a compressor. The super-heated vapour then exchanges heat

with water drawn from the cold well. This heats the water for storage in the hot well, and condenses the R134a to a saturated liquid at state 4. Finally, the R134a expands through the turbo-expander to return to state 5.

Figure 7 shows the operation of the modified heat pump cycle in the winter. In the winter, the cold mixed-phase R134a which exits the turbo-expander at state 5 is evaporated and super-heated using water drawn from the hot well. Just as it was in the summer, the super-heated vapour is mechanically compressed to state 3. The hot, super-heated vapour is then used for air and water heating in the home to fully condense the R134a to a saturated liquid. Finally, the R134a expands through the turbo-expander to return to state 5.

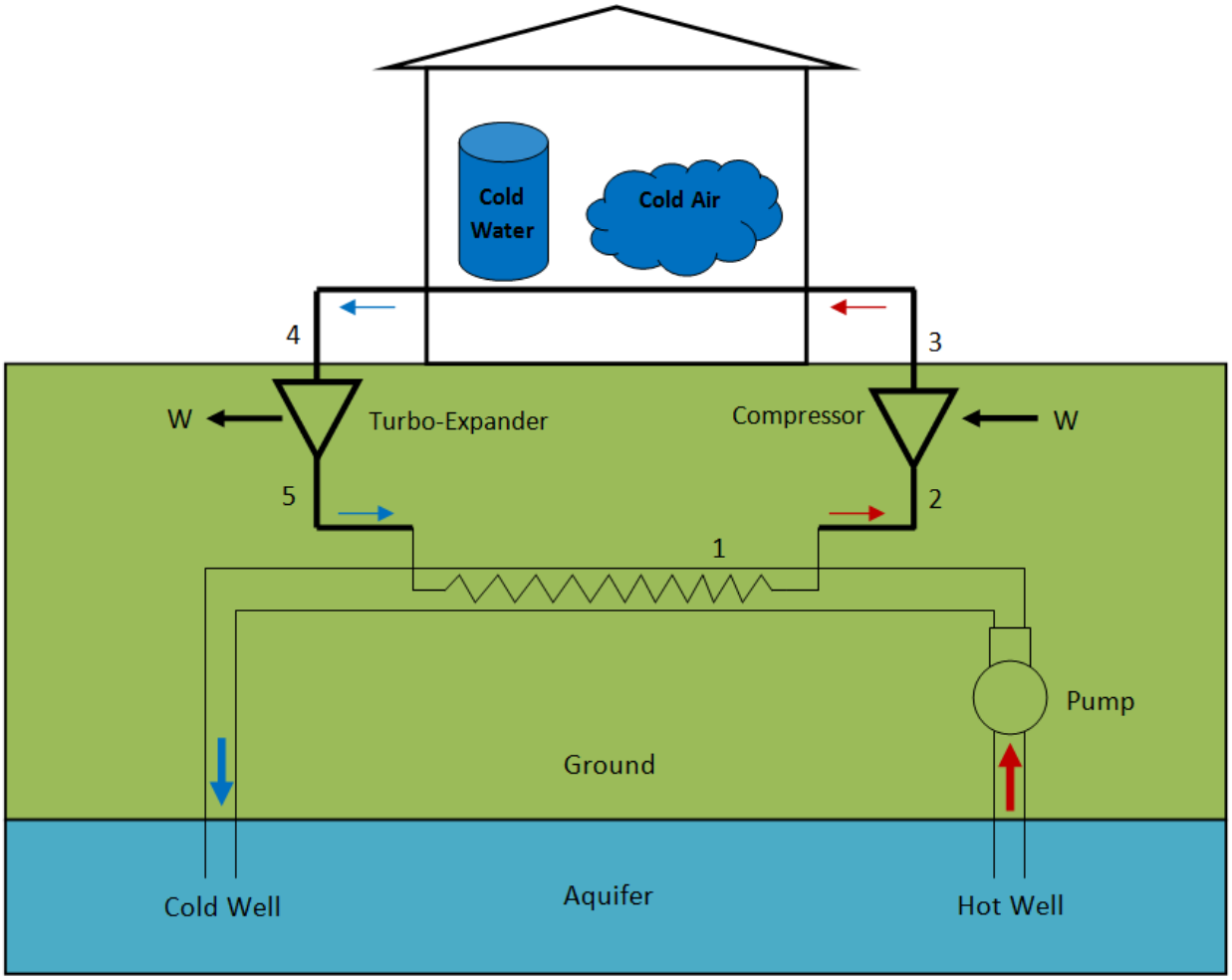

Figure 7 - Modified Heat Pump Cycle Operation in the Winter

2. Rankine Cycle

The operation of the Rankine cycle in the summer and winter is shown in Figure 8 and Figure 9, respectively. The Rankine cycle has a number of crucial differences from the modified heat pump cycle. The most notable is that in the Rankine cycle's operation in both seasons, heat is exchanged solely with the ambient and the cycle does not serve as a heat pump for the home. To examine the reason for this, consider the summer cycle. After the isentropic pumping process, the fluid leaves as a compressed liquid (state 2). Since the isobaric phase change of the R134a is also isothermal, nearly all of the heating of the R134a from state 2 to state 3 occurs at the maximum temperature of the R134a in the cycle. As such, the capacity of the fluid in state 2 for cooling purposes is practically non-existent. A similar limitation exists in the winter, whereby the R134a possesses nearly no heating capacity at state 4.

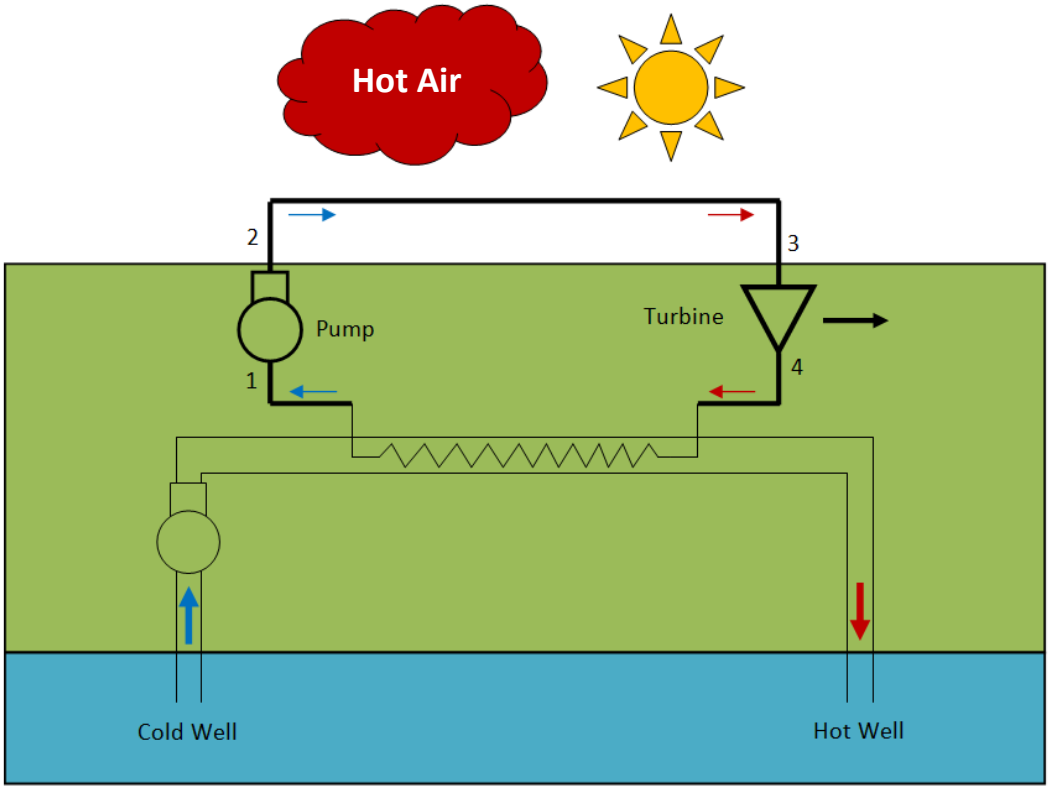

Figure 8 - Rankine Cycle Operation in the Summer

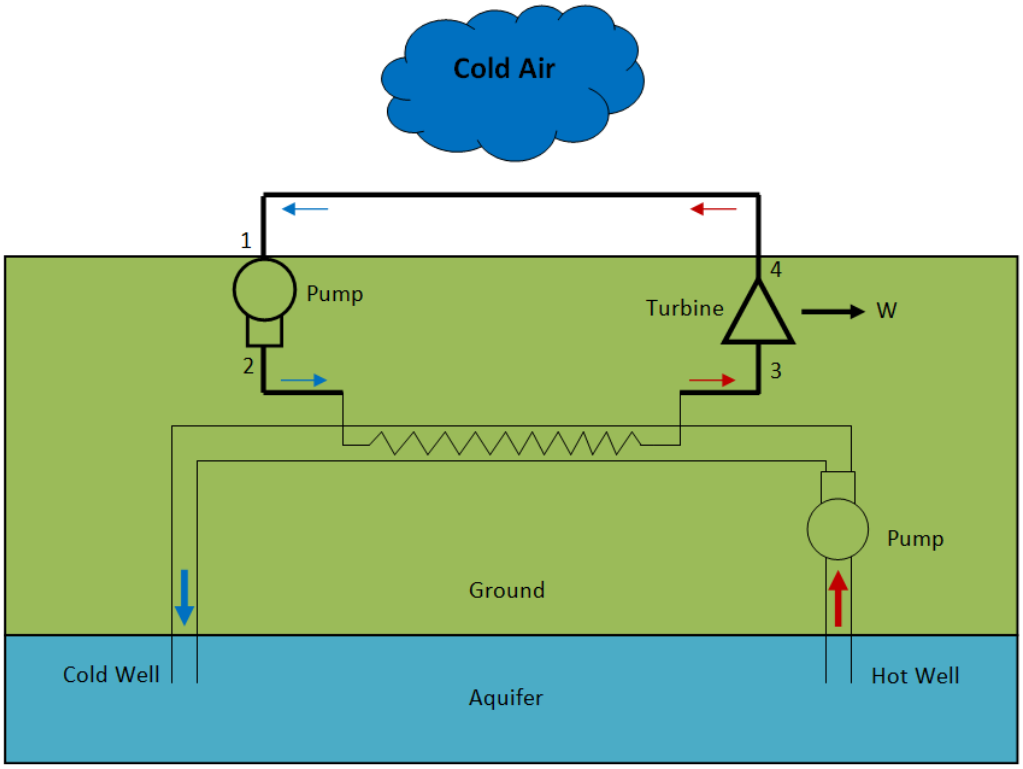

Figure 9 - Rankine Cycle Operation in the Winter

Another consequence of the Rankine cycle's property of evaporating the R134a at its hottest temperature and condensing it at its coldest temperature is that the temperature difference in the cycle is reduced, and the effectiveness of both heat exchange processes is also reduced. That`s because the effectiveness of the heat exchangers is proportional to the temperature difference between the R134a and ambient/water.

C. Heat Exchange Models

The following subsections provide the models for the four heat exchangers used in the modified heat pump cycle operation. These four heat exchangers are:

1. Water-R134a Concentric Counter-Flow Heat Exchanger
2. Air Duct-R134a Parallel-Flow Heat Exchanger
3. Water Heater-R134a Natural Convection Heat Exchanger
4. R134a Solar Collector

1. Water-R134a Concentric Counter-Flow Heat Exchanger

a) Geometry

Heat Exchange between the water and the R134a was modeled as a concentric, counter-flow heat exchanger.

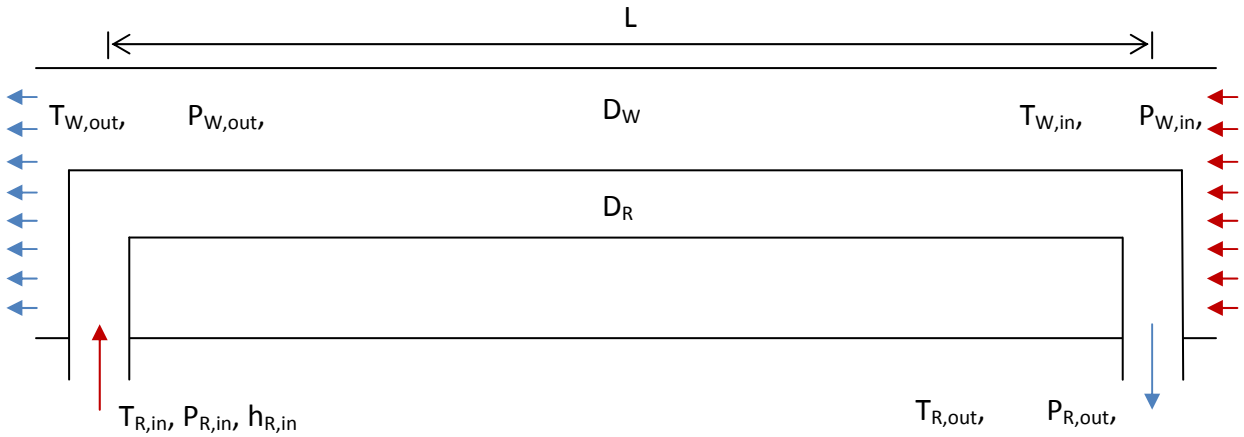

Figure 10 - Water-R134a Heat Exchanger Geometry

b) Assumptions

- Full Developed Flow
- No heat loss from the system (the water pipe is insulated)
- The refrigerant undergoes isothermal phase change
- No fouling of pipe walls in the heat exchanger
- Smooth Pipes

c) Analysis

The system will be analyzed using the Effectiveness-NTU Methodology described in [3]. The total heat transfer rate, q, is defined as:

$$q = \varepsilon C_{min}(T_{R,in} - T_{W,in})$$

Where ε is the effectiveness of the heat exchanger and C_{min} is:

$$C_{min} = \dot{m}_W c_{p,W}$$

C_{min} is defined by water because R143a undergoes an isothermal phase change. The effectiveness of the heat exchanger is defined by [3]:

$$\varepsilon = 1 - e^{-NTU}$$

Where the number of transfer units, NTU, is [3]:

$$NTU = \frac{UA}{C_{min}}$$

The overall heat transfer per unit temperature difference, UA, for the heat exchanger can be determined using the following relationship [3]:

$$\frac{1}{UA} = \frac{1}{h_W A_W} + \frac{\ln\left(\frac{D_{R,o}}{D_{R,i}}\right)}{2\pi k L} + \frac{1}{h_R A_R}$$

Where k is the conduction coefficient of the R134a pipe wall, and h_W and h_R are determined by the flow properties of the water and R134a, respectively. The heat transfer coefficient, h, is related to the Nusselt number through [3]:

$$h = \frac{Nu_D k}{D}$$

Gnielinski's relationship was used to determine the Nusselt number of the internal flow. This relationship was selected for its tolerance of near-transitional flow, and validity over a large range of Reynolds and Prandtl numbers ($3000 \leq Re \leq 5 \times 10^6$ and $0.5 \leq Pr \leq 2000$ respectively). Gnielinski's relationship for the Nusselt number is [3]:

$$Nu_D = \frac{(f/8)(Re_D - 1000)Pr}{1 + 12.7(f/8)^{1/2}(Pr^{2/3} - 1)}$$

Where the friction factor, f, can be found using Petukhov's correlation [3]:

$$f = (0.790 \ln Re_D - 1.64)^{-2}$$

The Reynolds number, Re, is defined as [4]:

$$Re_D = \frac{\dot{Q}D}{\upsilon A}$$

Where Q is the volumetric flow rate, v is the kinematic viscosity of the fluid and A is the cross-sectional area of the pipe.

2. Air Duct-R134a Parallel-Flow Heat Exchanger

a) Geometry

The Air-R134a heat exchanger was modeled as 12 pipes running parallel to the flow direction inside the HVAC duct.

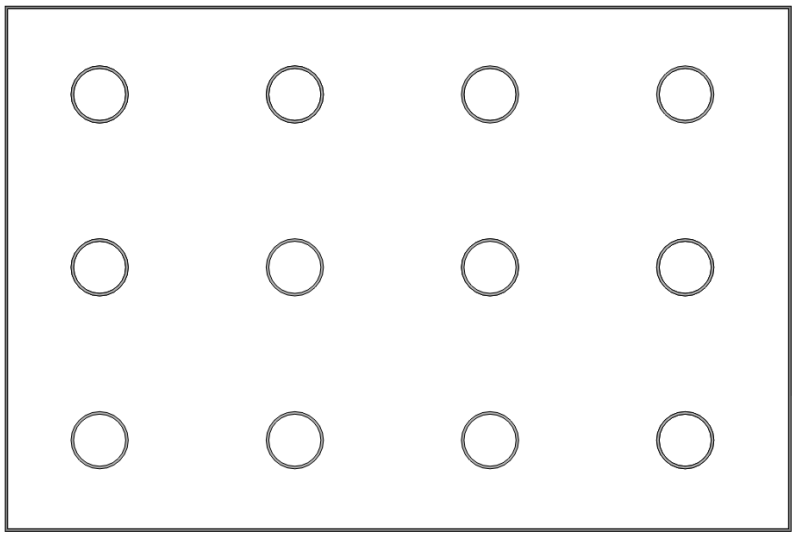

Figure 11 - Cross Section of Pipes Running Parallel to the Air Duct

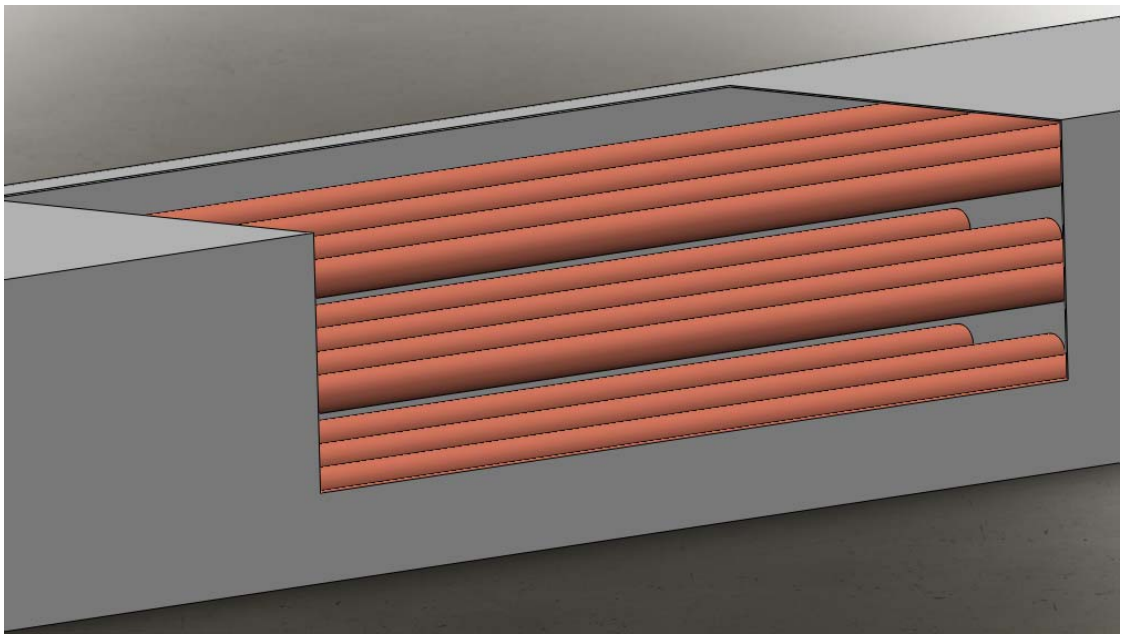

Figure 12 - Duct Wall Cut-Away to Reveal Copper Pipes Running Parallel to the Flow Direction

b) Assumptions

- Full Developed Flow
- No heat loss from the system (the duct is insulated)
- The refrigerant undergoes isothermal phase change
- No fouling of pipe walls in the heat exchanger
- Smooth Pipes

c) Analysis

The system can be analyzed using the same analysis methodology used for the Water-R134a Concentric Counter-Flow Heat Exchanger. This analysis remains applicable because the effectiveness, ε, of a heat exchanger with one fluid undergoing isothermal phase change is independent of geometry.

3. Water Heater-134a Natural Convection Heat Exchanger

a) Geometry

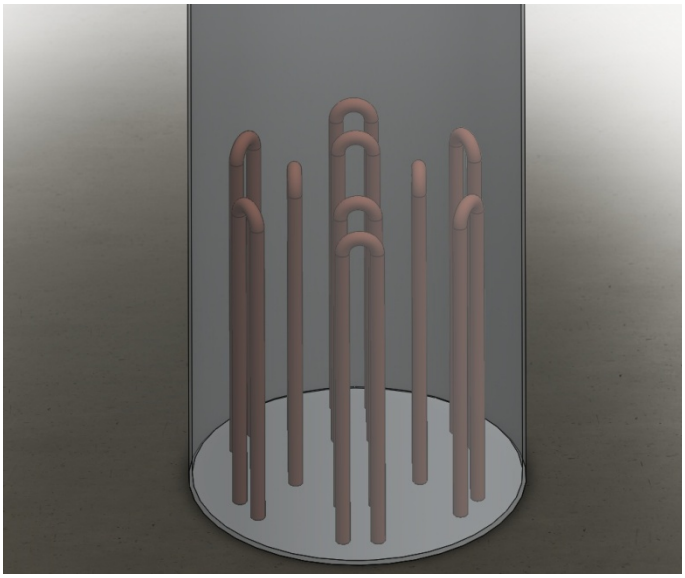

Figure 13 - Series of Vertical Pipe Loops Arranged at the Bottom of the Hot Water Tank

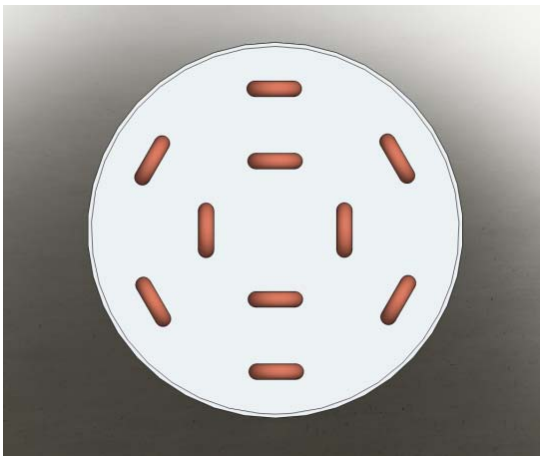

Figure 14 - Top View of the Vertical Pipe Loops in the Hot Water Tank

b) Assumptions

- Full Developed Flow
- No heat loss from the system (the duct is insulated)
- The refrigerant undergoes isothermal phase change
- No fouling of pipe walls in the heat exchanger
- Smooth Pipes

c) Analysis

The system can be analyzed using a similar analysis methodology used for the Water-R134a Concentric Counter-Flow Heat Exchanger and Air Duct-R134a Parallel-Flow Heat Exchanger. The relationship for the heat exchanger effectiveness in these analyses remain applicable because the effectiveness, ε, of a heat exchanger with one fluid undergoing isothermal phase change is independent of geometry.

The only difference with the analysis of the Water Heater-R134a Natural Convection Heat Exchanger is the heat transfer coefficient of the water, h_W. This heat transfer coefficient was determined by modeling the vertical R134a pipe loops as a vertically orientated wall which

experiences natural convection. The heat transfer coefficient is related to the Nusselt number through [3]:

$$h = \frac{Nu_L k}{L}$$

In [3], Churchill and Chu propose the following expression for the Nusselt number of natural convection of a vertical plate:

$$\overline{Nu}_L = \left\{0.825 + \frac{0.387{Ra_L}^{1/6}}{[1 + (0.492/Pr)^{9/16}]^{4/9}}\right\}^2$$

Where the Rayleigh number, Ra, is defined as [3]:

$$Ra_L = \frac{g\beta(T_s - T_\infty)L^3}{\nu\alpha}$$

Where β is [3]:

$$\beta = -\frac{1}{\rho}\left(\frac{\partial\rho}{\partial T}\right)_P \approx -\frac{1}{\rho}\frac{\rho_\infty - \rho}{T_\infty - T}$$

4. R134a Solar Collector

a) Geometry

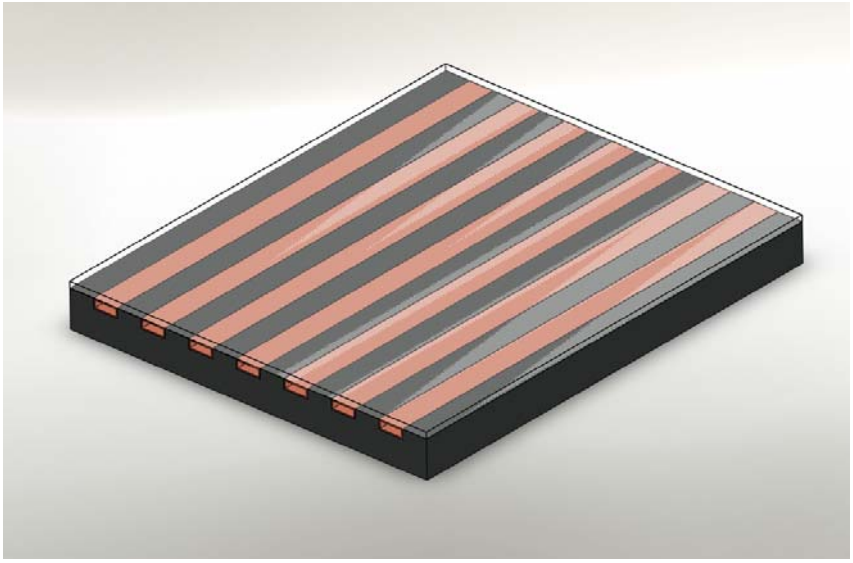

Figure 15 - R134a Solar Collector Model Geometry

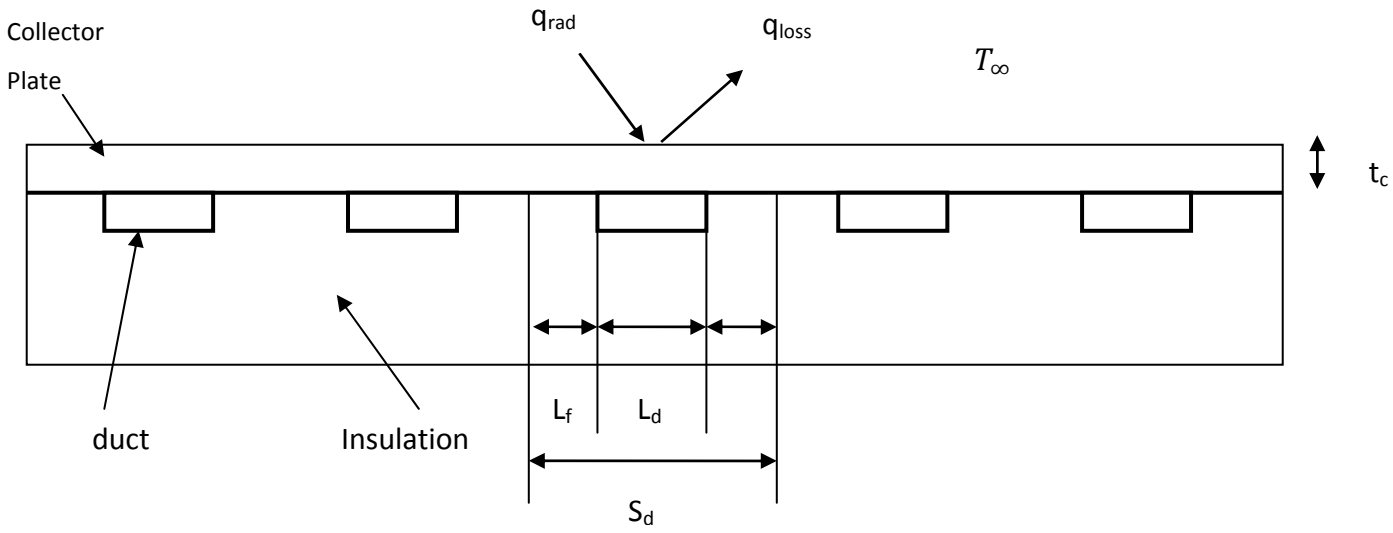

Figure 16 - Cross Section of R134a Solar Collector [5]

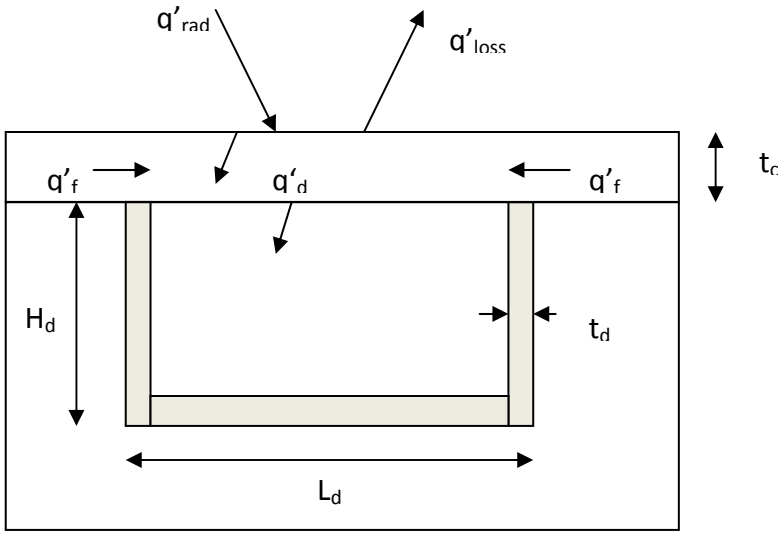

Figure 17 - Enlargement of a Single Duct in the R134a Solar Collector [5]

b) Assumptions

- Steady State conditions
- No heat loss through the sides or bottom of the plate
- No interaction between the ducts
- Constant temperature, T_b, maintained at the base of the "fin"
- Fully developed flow within the duct

c) Analysis

The analysis of the R134a Solar Collector was adapted from Leverick and Olmstead's work in [5]. The analysis is divided into three section; the fin analysis, the duct analysis and an overall analysis.

(1) Fin Analysis

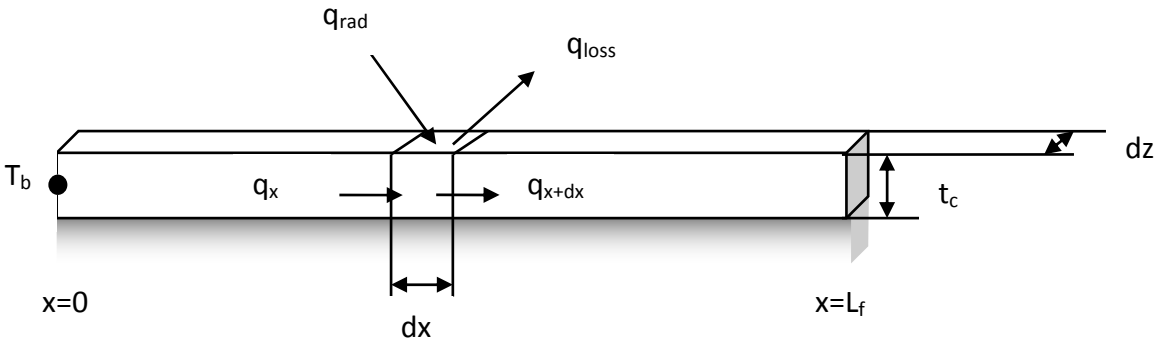

Figure 18 - Fin Analysis of the R134a Solar Collector [5]

An energy balance yields:

$$q_{rad} + q_x - q_{loss} - q_{x+dx} = 0$$

Plugging in and rearranging results in [3]:

$$\frac{d^2T}{dx^2} - \frac{U_C}{kt_C}\left[T - \left(T_\infty + \frac{q''_{rad}}{U_C}\right)\right] = 0$$

Employing the solution for a case B fin yields [3]:

$$q'_f = 2U_c L_f \eta \theta_b$$

(2) Duct Analysis

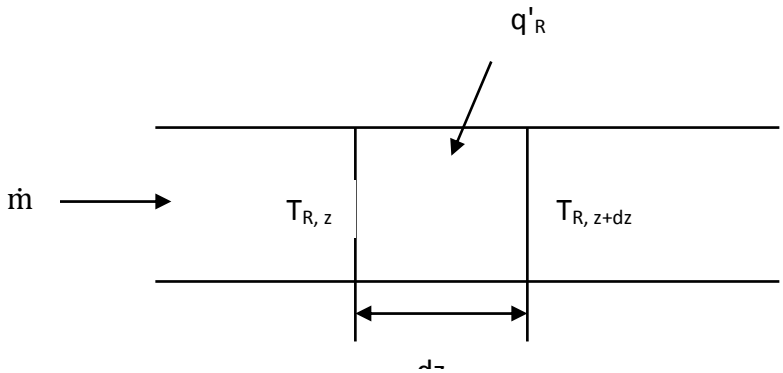

Figure 19 - Duct Analysis of the R134a Solar Collector [5]

An energy balance yields:

$$q'_R dz + \dot{m}_R c_p T_{R_z} - \dot{m}_R c_p T_{R_{z+dz}} = 0$$

Simplifying and solving results in [3]:

$$q'_R = \dot{m}_R c_p \frac{dT_R}{dz}$$

(3) Overall Analysis

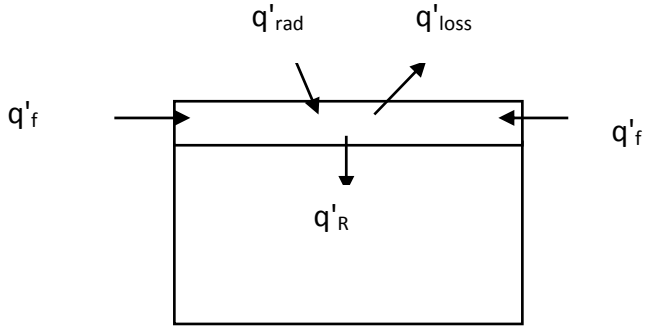

Figure 20 - Overall Analysis of the R134a Solar Collector [5]

Energy balance yields:

$$q'_R = q''_{rad} L_d - U_C L_d (T_b - T_\infty) + 2U_c L_f \eta \theta_b$$

Heat transfer to the water gives:

$$q'_R = h_i A_i (T_b - T_R)$$

Combining and solving yields:

$$q'_R = S_d \left(\frac{\frac{1}{S_d U_c}}{\frac{1}{hA} + \frac{1}{U_C (L_d + 2\eta L_f)}} \right) \left(q''_{rad} - U_C (T_R - T_\infty) \right)$$

Using the solution from the duct analysis separating variables and integrating yields:

$$\frac{T_{R_o} - \tilde{T}_\infty}{T_{R_i} - \tilde{T}_\infty} = exp \left(-\frac{S_d U_C}{\dot{m} c_p} \left(\frac{\frac{1}{S_d U_c}}{\frac{1}{hA} + \frac{1}{U_C (L_d + 2\eta L_f)}} \right) w_c \right)$$

The heat transferred to the water for one duct would be:

$$q_R = \dot{m} c_p \left(T_{R_o} - T_{R_i} \right)$$

D. Pressure Loss Model

The pressure loss incurred by the R134a as it passes through the heat exchangers determines the outlet pressure of the R134a. The total pressure loss is a result of the major and minor losses in the piping [4]:

$$P_2 - P_1 = \frac{\rho}{g}(h_l + h_{l.m})$$

Where the major losses (resulting from friction in the pipe walls) are [4]:

$$h_l = f\frac{L}{D}\frac{\bar{V}^2}{2}$$

Where f is the friction factor, L is the length of pipe and D is the diameter of the pipe. The average flow velocity, V, is:

$$\bar{V} = \frac{\dot{m}}{\rho A}$$

Minor losses are the result of various fittings and bends in the piping. These are [4]:

$$h_{l,m} = f\frac{L_e}{D}\frac{\bar{V}^2}{2}$$

Where the equivalent length, L_e/D, is a factor associated with the type of fitting.

E. Modified Heat Pump Cycle Analysis Methodology

In order to analyze the cycle, the state of the fluid will be assumed at the inlet of the compressor (state 2). The state of the fluid will then be calculated as it proceeds through the cycle. The geometries of the heat exchangers and operating conditions of the turbine and pump will be adjusted to return the fluid to its initial state when it reaches the inlet to the turbine. In a real-world operable system, the loading conditions of the turbo-expander and compressor would be adjusted by a control system to maintain the proper cycle operation.

F. Cycle Calculations

A sample cycle calculation will be performed for the winter and summer cycles to demonstrate the assumptions relating to non-ideal state changes and show the power and heating outputs of the cycle in two different states. All thermodynamic properties of R134a were obtained from DuPont's technical document on HFC-134a [6]. All intermediate values are obtained using linear interpolation. The results for the calculations in summer are presented in TABLE II. The results calculations for the winter season, as well as detailed calculations for both seasons, are presented in Appendix C.

TABLE II: RESULTS FOR STATE PROPERTIES DURING THE SUMMER

State	Parameter	Value	Units
Initial	T_2	70	℃
	P_2	1800	kPa
	h_2	437.4	kJ/kg
	s_2	1.7306	$kJ/kg°K$
	v_2	0.01134	m^3/kg
Compression	T_3	96.7	℃
	P_3	2800	kPa
	h_3	452.7	kJ/kg
	s_3	1.7481	$kJ/kg°K$
	v_3	0.00722	m^3/kg
Condenser	T_4	82.9	℃
	P_4	2792.7	kPa
	h_4	328.5	kJ/kg
	s_4	1.4005	$kJ/kg°K$
	v_4	0.0011	m^3/kg
Turbo-expander	T_5	-15	℃
	P_5	163.9	kPa
	h_5	310.2	kJ/kg
	s_5	1.4291	$kJ/kg°K$
	x_5	0.620	Unitless

Determining the efficiency of the cycle is difficult because the system serves two purposes; to generate power and to operate as a heat pump. The efficiency was calculated using the following equation:

$$\eta = \frac{Energy\ Desired}{Energy\ Input} = \frac{W_{out} + Q_{heat\ pump}}{W_{Compressor} + W_{Pump}}$$

TABLE III summarizes the power and heat flow results from the case study.

TABLE III: SUMMARY OF CASE STUDY RESULTS

Power	**Summer**	W_{out}	31.11 kW
		$W_{Compressor}$	26.01 kW
		W_{Pump}	3.0 kW
		W_{net}	2.1 kW
	Winter	W_{out}	37.6 kW
		$W_{Compressor}$	29.5 kW
		W_{Pump}	3.0 kW
		W_{net}	5.1 kW
Heat Pump Output	**Summer**	$Q_{Air\ Conditioning}$	13.53 kW
	Winter	$Q_{Air\ Heating}$	33.7 kW
		$Q_{Water\ Heating}$	129.7 kW
Heat Storage	**Summer**	Q	212.7 kW
	Winter	Q	205.3 kW
Cycle Efficiency	**Summer**	η	153.9%
	Winter	η	518.5%

VI. Thermal Energy Storage

In order for the heat pump system to be effective during all seasons, it is necessary to design a system to store thermal energy. While there are a number of techniques available for storing heat, the mechanism to be used in this design is an aquifer thermal energy storage (ATES) system. This technique was chosen due to the presence of easily accessible aquifers beneath the city of Winnipeg, as well as based on recommendation by the client. In order to perform an analysis and develop a design for the ATES system, a considerable amount of information on the nature of aquifers in general, and the Winnipeg aquifer specifically, are needed. This information will be presented in subsections A and B.

A. Introduction to Aquifers and Aquifer Properties

Before an aquifer thermal energy storage system can be designed, it is necessary to understand the nature of aquifers and to define some properties of aquifers, which will be used to describe the hydraulic and thermal behavior of the groundwater. There are a number of geological formations which store ground water, but an aquifer is a special type of formation. Only formations which are capable of transmitting a sufficient flow of water to supply a well or spring are classified as aquifers [8]. Aquifers consist of a porous medium, called the matrix, which is usually sand, gravel, or rock such as limestone, which is highly fractured. Water diffuses through cracks and pores in the ground, where it eventually reaches the aquifer. The volume of water contained within an aquifer, the flow rate of that water and the heat transfer properties of groundwater all depend on the properties of the individual aquifer.

The most fundamental property which defines the volume of water stored within an aquifer is called porosity, and is a measure of the volume of voids in a geological formation. In the case of sand and gravel aquifers, the porosity is directly associated with the space between the

individual grains in the matrix. In the case of a fracture rock aquifer, the porosity is a combination of the porosity in the matrix and the number of fractures in the rock. In a fractured rock aquifer, especially limestone and sandstone aquifers, the porosity is often time dependent, as erosion and mineral deposition have a significant effect on the size of pores and fractures [9].

Another critical property of the aquifer is the hydraulic conductivity. Hydraulic conductivity is a measure of the volumetric flow rate of water as it travels through the aquifer [8]. The hydraulic conductivity is also often expressed as a parameter called permeability. Permeability differs from hydraulic conductivity in that the permeability depends only on the properties of the medium, while hydraulic conductivity applies to water flow through the medium. Permeability can be expressed as hydraulic conductivity using an equation derived from Darcy's Law:

$$K = \frac{\kappa \rho g}{\mu}$$

where κ is the permeability, ρ is the density of the fluid, μ is the dynamic viscosity and g is the acceleration due to gravity [10].

The hydraulic conductivity can be estimated using analytical methods although it is often similar to determine the value experimentally at the well site. One such method is called the Pump Test, which involves pumping water out of the aquifer under known pressures and increasing the flow rate until the aquifer can no longer transmit the desired flow [11]. The hydraulic conductivity is important for several reasons, including the draw and injection of water, as well as the natural flow rate of the water in the aquifer.

Since heat is being stored in the aquifer, the thermal properties of the aquifer must also be determined. The two properties associated with heat transfer in an aquifer are the thermal conductivity and the specific heat capacity. The thermal conductivity is a measure of the

amount of heat that conducts through a material, while the heat capacity is a measure of the amount of energy needed to raise the temperature of a certain mass of material. These quantities are highly dependent on the aquifer under consideration, as the properties of the individual rock constituents and water mineral content will ultimately determine the thermal properties.

The internal pressure in the aquifer is the result of the hydraulic gradient, gravitational potential and possibly buoyancy effects. The pressure in the aquifer is defined in terms of point-water head, which is defined as:

$$h_{ip} = z + \frac{P}{\rho g}$$

where z is the height of the water surface above the measuring instrument, p is the pressure, ρ is the water density at the surface, and g is the gravitational constant.

B. Properties of the Winnipeg Aquifer

The aquifer underneath Winnipeg, extends across much of Southern Manitoba, and will be referred to for the remainder of the paper as the Winnipeg Aquifer. The geology of the Winnipeg Aquifer varies considerably, not only laterally, but also vertically as can be seen in the cross section of the aquifer found in Figure 21.

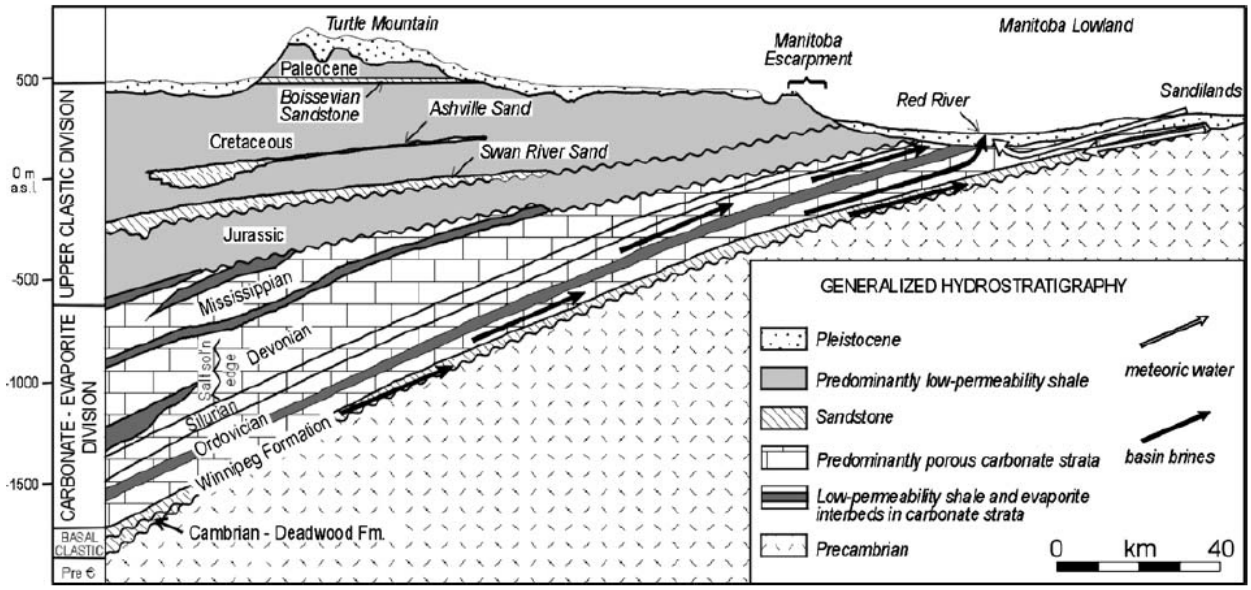

Figure 21: Cross section of Winnipeg Aquifer demonstrating layers and direction of water flow. [12]

It can be seen that, while there is considerable variation in thickness, depth and geological formation, that in the area around the Red River on the right side of Figure 21, the structure is relatively uniform. In fact, to the East of the Red River, where the proposed design is intended to be installed, the aquifer geological formation is quite simple. At the very top is the Pleistocene layer, which is composed primarily of glacial deposits. Beneath the Pleistocene layer is a thick carbonate formation called the Carbonate Rock Aquifer. The Carbonate Rock Aquifer can be divided into three levels called the Upper, Middle and Lower Carbonate Formations, each of which with different properties. Underneath the Carbonate Rock Aquifer is a sandstone aquifer called the Winnipeg Formation, which overlays the bedrock, called the Precambrian shield.

In the Winnipeg region, the upper region of the aquifer is highly fractured, and thus has a high permeability and storage capacity. The middle region has only a small amount of fracturing, resulting in low permeability while the lower region exhibits properties similar to the upper region, though with a lower degree of fracturing. A representative model of how the aquifer might look can be found in Figure 22.

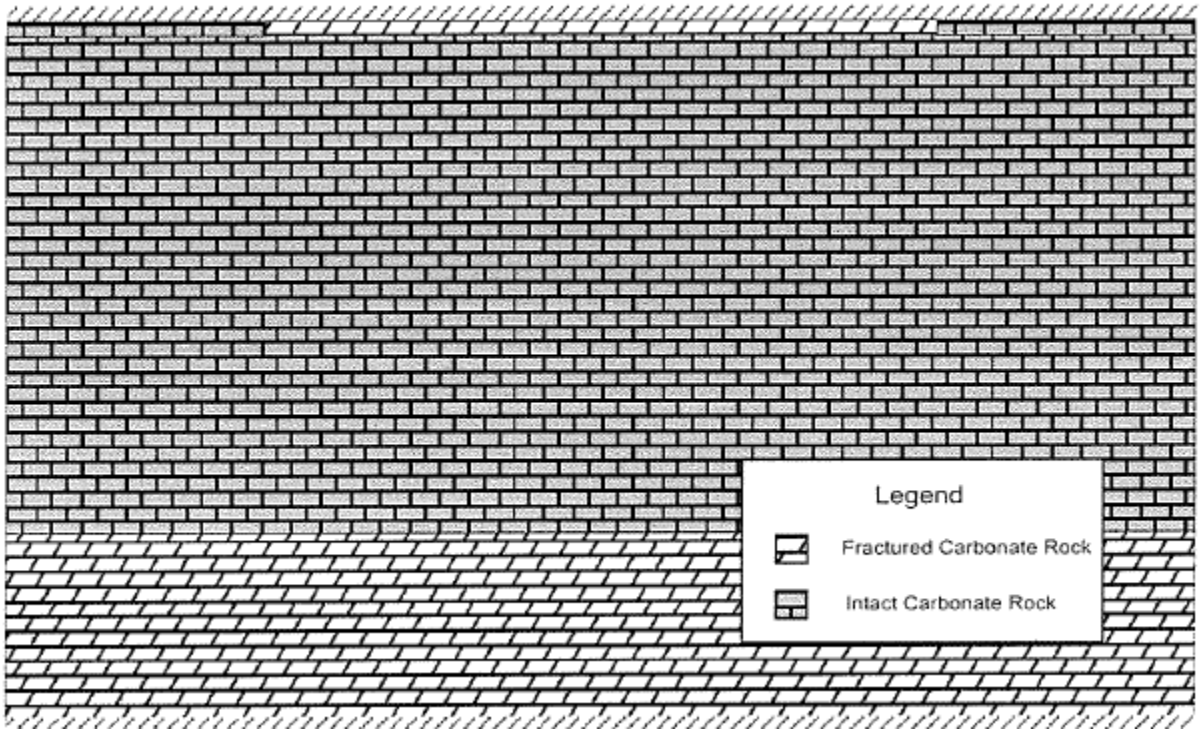

Figure 22: Representation of layering and degree of fracturing in Carbonate Rock Aquifer [13]

The brick-like representation of the carbonate strata is not an arbitrary one. The carbonate layers are laid out in bedding planes, joints between the rocks, just as is shown in Figure 22 [13]. While such a degree of symmetry is unlikely in the actual aquifer, the presence of bedding planes and joints contributes to matrix porosity, and thus the permeability of the aquifer.

Since the proposed system is intended to operate in the Winnipeg area, a magnification of Figure 21, emphasizing the Winnipeg region is presented in Figure 23.

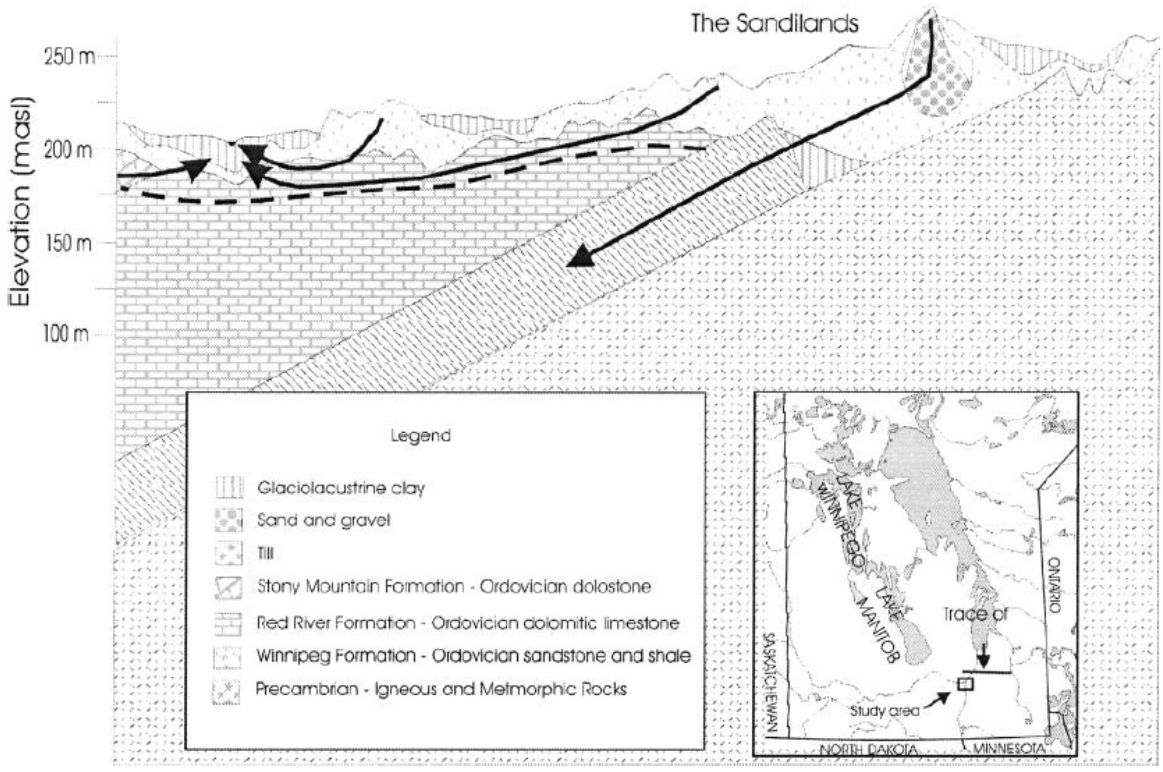

Figure 23: Magnification of Figure 21 with emphasis on the Winnipeg region. [14]

There are several interesting points to note with regard to the water flows shown in Figure 21 and Figure 23. It can be seen that the water flows from two different directions and that these two flows merge in the vicinity of the Red River. The flow from the East is meteoric or fresh water and the flow from the West is brine, or salt water. Thus, it is important which side of the river the system is placed on, as different procedures and equipment may be necessary for handling the flow of brine. The direction of water flow in the Winnipeg Aquifer can be found in Figure 24.

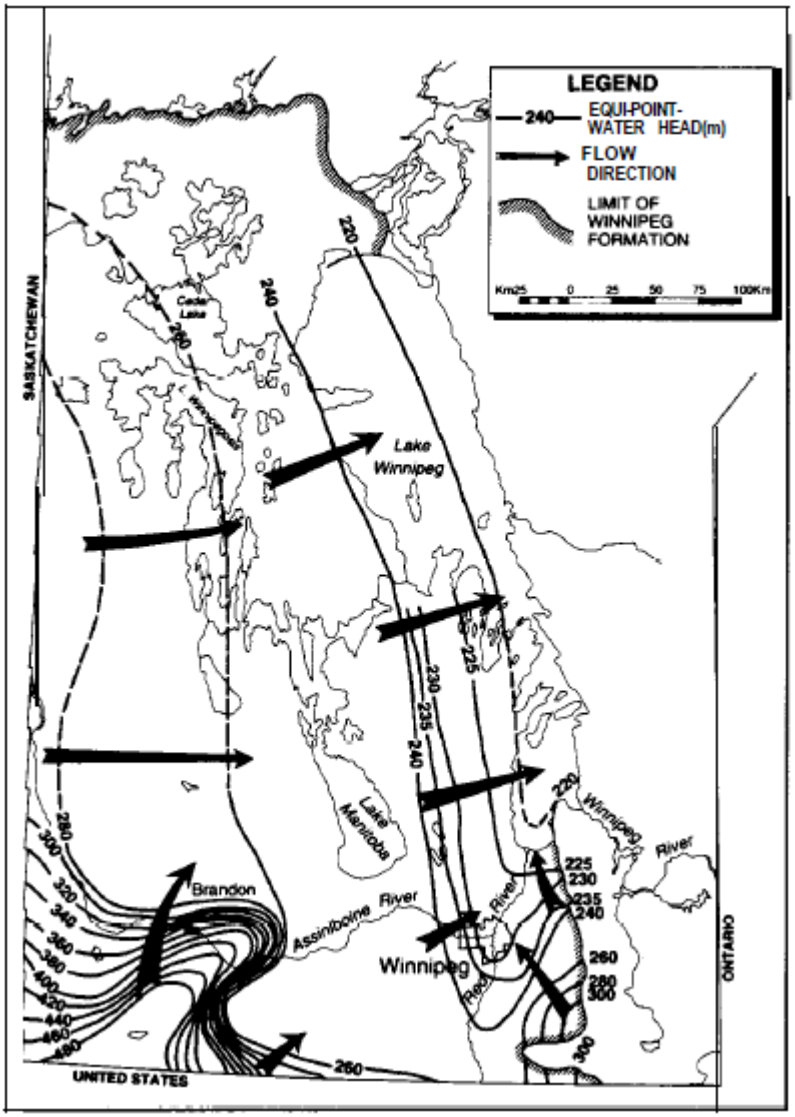

Figure 24: Flow directions and point-water heads in Winnipeg Aquifer [15]

Figure 24 also contains data regarding the water pressure in the aquifer. In the Winnipeg region, the aquifer water pressure is approximately 230 (m), and is independent of whether the flow under consideration is fresh or brackish water.

With the nature of the Winnipeg Aquifer introduced, the properties of the aquifer have been summarized in TABLE IV for the Carbonate Rock Aquifer, which is more likely to serve the needs of the proposed system than the other aquifers in the Winnipeg Region [13].

TABLE IV: TABLE OF PROPERTIES FOR THE WINNIPEG AQUIFER [12], [13]

Property	Aquifer Level	Value	Metric
Aquifer Material		Limestone, Dolomite	N/A
Depth*	Upper	45	m
	Lower	135	m
Thickness	Upper	15	m
	Lower	25	m
Transmissivity	Upper	620	$\frac{m^2}{day}$
	Lower	620	$\frac{m^2}{day}$
Maximum Permeability**	Upper	5.0×10^{-8}	m^2
	Lower	1.0×10^{-9}	m^2
Average Permeability	Upper	1.0×10^{-11}	
	Lower	1.0×10^{-11}	
Hydraulic Gradient		3.0×10^{-4}	Unitless
Matrix Porosity	Upper	0.1	Unitless
	Lower	0.1	Unitless
Fracture Porosity**	Upper	0.05	Unitless
	Lower	0.005	Unitless
Total Porosity***	Upper	~0.25	Unitless
	Lower	~0.20	Unitless
Point Pressure Head†		230	m
Initial Temperature	Upper	7	°C
	Lower	8.3	°C
Thermal Conductivity		2.4	$\frac{W}{m\,K}$
Heat Transfer Rate‡		84×10^{-3}	$\frac{mW}{m^2}$

*Depths measured at the bottom of each level
** Average values (can be significantly higher or lower due to presence of large cavern type voids)
† Determined for entire aquifer at the base of the Winnipeg Formation (Beneath Lower Carbonate Aquifer)
‡ Measured in an aquifer of similar geological and thermal properties

C. Design Considerations

With the aquifer properties in the Winnipeg region known, it is now possible to design the individual components of the aquifer thermal energy storage system. The basic system was described in the introduction of this report. The system consists of two wells separated by a certain distance and drilled down to a certain depth in the aquifer. Each well is to be able to both draw and inject water into the aquifer, and one well is to store heat while the other stores cold. It is required that the system be able to recover as much heat or cold as possible, and that, since the system is intended for installation in a residential property, that the system be designed to be as cost effective as possible. The first stage in this process is to lay out the assumptions that are to be made in the subsequent analysis, followed by the introduction of the various design considerations and the design decisions made based on those consideration.

1. Assumptions

Only heat transfer from the hot fluid to the cooler aquifer will be assessed. This is done because the temperature difference in the region of the hot well is much larger than the temperature difference in the region of the cold well. Thus, if the heat transfer is small for the hot well, it will be even smaller for the cold well.

When water is injected into the aquifer, some of the energy is needed to heat the rack strata and water already present in the aquifer. However, due to the low heat flow rate in the aquifer, once the rock has been heated, the energy lost to this heating will be much lower in subsequent years. Thus, it was assumed that the aquifer is being studied a number of years after installation, when the system has reach a state of equilibrium.

As the water is being stored in the aquifer, heat will conduct to the surrounding aquifer, and the temperature of the water will subsequently change. This makes the problem highly

transient. To simplify the analysis, it is assumed that no heat transfer occurs during the injection period, and that during the storage phase, heat transfer occurs as if no fluid is being drawn out.

2. Draw Down and Water Displacement

Since water is being both drawn out of and injected back into the aquifer, the issue of where the water comes from during pumping and where it goes during injection must be taken into consideration. During pumping of water from an open vessel, the water level would drop uniformly along the surface, since there would be no obstruction to fluid flow. However, in an aquifer, the hydraulic conductivity defines a maximum flow rate within the aquifer. Thus, as water is being pumped out of the aquifer, the surrounding aquifer cannot recharge the water as quickly as it is removed. This results in the draw down pattern shown in Figure 25

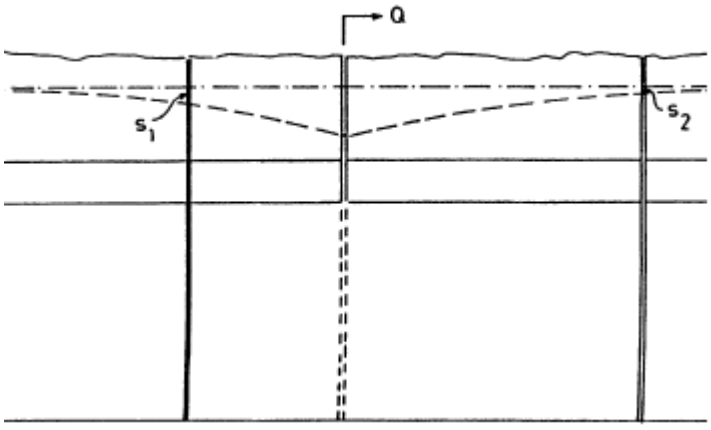

Figure 25: Schematic representation of drawdown denoted as s1, s2 [16]

If the drawdown slopes beneath the water level of the pump, the system will stall, as the pump would no longer be submerged. However, systems already in use in the Winnipeg area for groundwater cooling are able to draw $13\ \left(\frac{L}{s}\right)$ for 8 hours a day, implying that aquifer would be

capable of supplying a continuous flow of approximately $4.25\ \left(\frac{L}{s}\right)$ without stalling the pump [13].

When water is injected, there are two forces acting on it as it enters the aquifer. The pressure supplied by the pump and buoyancy both act on the water and influence the flow. Thus, water initially flows outwards from the pressure and upwards due to buoyant effects. The resulting shape would then look very similar to the drawdown cone. However, in order to inject water, the water already present needs to be displaced. Since this displacement would increase the groundwater pressure, and hence the flow rate, this displacement would have to be carried out over a number of seasons in order to not damage the aquifer. However, eventually, a state of equilibrium would be reached, and the water would no longer need to be displaced from the aquifer during injection.

3. Aquifer Selection and Well Depth

Selection of the borehole depth depends both on the nature of the aquifer under consideration, as well as the flow properties expected at the inlet and outlet of the pipes. There are two broad scale requirements for the aquifer to meet the needs of the design. The aquifer must be large enough to supply and store the required volume of water and the temperature of the ground must be sufficiently steady that it can be considered to be at a constant temperature throughout the year. This constant temperature occurs at a depth of between 30 to 40 meters [17]. As a result, the borehole must be drilled past the Pleistocene layer and into the Carbonate Rock Aquifer, implying that the Carbonate Aquifer will serve as the storage medium.

Another problem to consider when selecting the depth of the borehole is the drawdown and injection issues presented above. Since the middle carbonate region has a small permeability, water should flow upwards towards the Upper Carbonate Aquifer in only small quantities. As such, the Winnipeg Aquifer should behave in some ways like a contained aquifer, meaning that the drawdown will be limited to the lower aquifer. Therefore, the borehole should be drilled nearly to the base of the Lower Carbonate Aquifer in order to ensure minimize the effects of drawdown.

4. Subsurface Pressure

The internal pressure in the aquifer is of importance because it determines the pump head required to remove water from the ground. Since the supplied data was measured at the base of the aquifer, the height of the aquifer must be measured to that point. When the thickness of the Winnipeg Formation is taken into consideration, the resulting pressure is between 200 and 300 (kPa). This is a relatively low pressure, meaning locating a suitable pump should not be difficult.

5. Subsurface Flow Rate and Well Alignment

In order for the ATES system to be effective, the water must remain in the vicinity of where it was injected into the well. Thus, it is important to demonstrate that the velocity of the groundwater is low.

The groundwater velocity is defined as:

$$v_{flow} = K\left(\frac{dh}{dl}\right)$$

Where K is the hydraulic conductivity and $\left(\frac{dh}{dl}\right)$ is the hydraulic gradient [8]. When this calculation is performed, the result is $v_{flow} = 1.985\left(\frac{m}{year}\right)$ or $v_{flow} = 0.993\left(\frac{m}{6\,months}\right)$. Since this value is relatively low, the effect of groundwater flow is not critical.

In order to ensure that the water flow from one well has minimal impact on the water stored in the other well, the wells will be aligned to negate the effect of water flow. By aligning the wells such that direction of flow is perpendicular to a line joining the two wells, the thermal interference resulting from groundwater flow will be minimized. A schematic of the orientation of the wells can be seen in Figure 26.

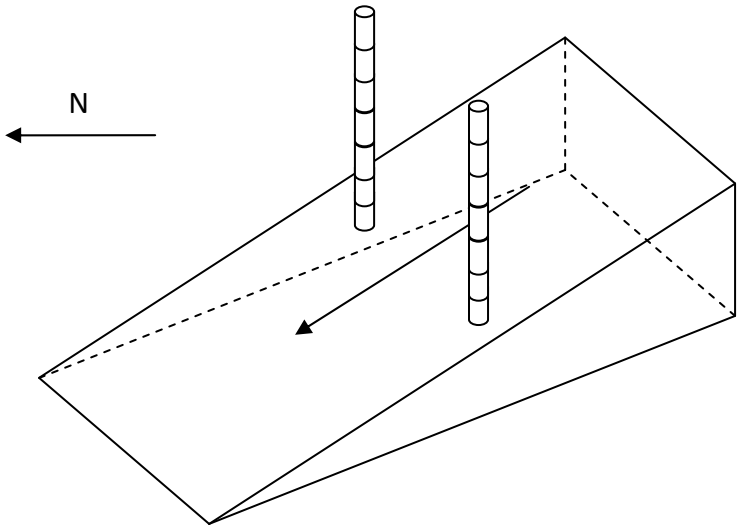

Figure 26: Well alignment considering flow direction

6. Thermal Losses and Well Separation

Since heat is being injected into a region of lower temperature, heat transfer will occur from the warm water to the cooler water and rock in the aquifer. In order to assess the temperatures of the fluid and rock in the aquifer, the properties of the mixture must be

determined. The properties of the individual components of the aquifer, neglecting constituents of smaller quantity, can be found in TABLE V.

TABLE V: THERMAL PROPERTIES OF PRIMARY AQUIFER CONSTITUENTS [17]

Property	Mass Specific Heat Capacity	Volumetric Heat Capacity	Density	Thermal Conductivity
Unit	$\frac{kJ}{kg\,℃}$	$\frac{kJ}{m^3\,℃}$	$\frac{kg}{m^3}$	$\frac{W}{m\,℃}$
Water	4.187	4187	999.52	0.605
Limestone	1.2	3285	2691.01	3.0
Dolomite	0.88	2510	2851.19	5.0

Since the porosity of the aquifer can be estimated, and this value is expressed as percent volume, the bulk properties can be estimated by the following:

$$c_{P_A} = \theta(1-\phi)c_{P_D} + \theta(1-\phi)c_{P_L} + \phi c_{P_W}$$

$$c_{P_R} = \theta c_{P_D} + \theta c_{P_L}$$

for the rock combined with water and for rock without water [13]. In these equations, θ is the percent fraction of dolomite with respect to limestone, ϕ is the porosity of the aquifer, and the terms denoted c_P represent the volumetric heat capacities of the individual components. Since these equations hold for any parameter expressed in volumetric terms, these equations can be applied to the bulk density as well. The results of these calculations can be found in TABLE VI.

TABLE VI: HEAT CAPACITIES AND DENSITY OF AQUIFER

Property	Value
Density	2416.17 $\left(\frac{kg}{m^3}\right)$
Volumetric Heat Capacity (Aquifer)	3284.35 $\left(\frac{kJ}{m^3\ ^\circ C}\right)$
Volumetric Heat Capacity (Rock)	2897.50 $\left(\frac{kJ}{m^3\ ^\circ C}\right)$
Mass Specific Heat Capacity	1.3590 $\left(\frac{kJ}{kg\ ^\circ C}\right)$

Since water in the aquifer is stored in a porous medium, the volume of water stored in the aquifer must be determined. The required water flow rate for the heat pump mentioned above is 25 gpm (Leave as gallons per minute, that will be fine). Using an aquifer thickness of 25 (m), the volume of water being stored can be determined from:

$$V = \pi R^2 h$$

where R is the radius of water “cylinder” and h is the thickness of the aquifer. These calculations follow from the assumption that the combination of water and rock will result in a cylindrical shape. While it has been mentioned that this is not the case, this assumption significantly simplifies the analysis. Furthermore, since the radius of thermal water in the aquifer will be smaller than R at the base of the aquifer and larger at the top, the cylindrical shape can be taken to serve as an average radius, as shown in Figure 27.

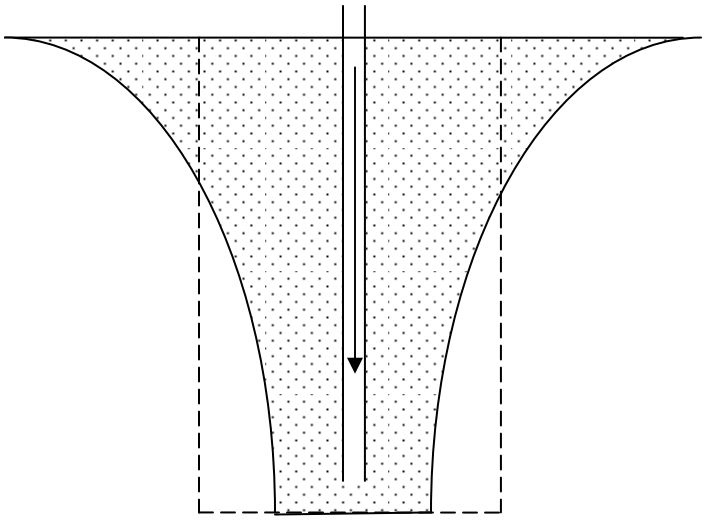

Figure 27: Average thermal storage region radius

Since the aquifer has a high percentage of rock and the water must fill the fractures and pores in the rock, the total volume of the structure can be defined as:

$$V_{Tot} = \frac{V_{Water}}{\phi}$$

where, once again, ϕ is the total aquifer porosity. This calculation results in a total water volume, over a six month period, of $24572.16\ m^3$ and the total volume of the water and rock combination was found to be $122860.8\ m^3$. The radius of the combination of rock and water was then determined to be $39.55\ m$.

The heat transfer can now be separated into the two possible heat flows. First, the temperature drop and heat losses in the water will be assessed, followed by the temperature increase in the surrounding aquifer, including rock and water.

As the volume of and heat capacity of the water is so large, the analysis will begin with a calculation using the Lumped Capacitance Method. The equation derived for this method was derived using an energy balance under the assumption that the volume being cooled remains at

the same temperature throughout the cooling. In other words, there is no temperature gradient within the mass of heated water and rock. This equation, as derived from its source [3] was derived using convection as the exterior heat transfer mode. Thus, since the primary mode of heat transfer under consideration is conduction, the equation was modified for this purpose and is presented as follows:

$$\frac{T(t) - T_\infty}{T_i - T_\infty} = exp\left[-\left(\frac{kA_S}{h}\right)\left(\frac{1}{\rho V c_P}\right)t\right]$$

In the above equation, T(t) represents the time varying temperature of the entire formation, T_i is initial temperature, T_∞ is the temperature of the non-storage region of the aquifer, k is the thermal conductivity, A_S is the surface area of the region being cooled, h is the aquifer thickness, ρ is the density, V is the volume, c_P is the specific heat capacity and t is the time of exposure [3]. This calculation, which can be found in Appendix D, results in a final temperature, after a six month period, of $58.82\ ℃$. This result indicates an astounding degree of thermal efficiency in the aquifer.

However, it might be expected that the temperature of the stored thermal water would be lower after such a lengthy period of time. Since this may have been the result of the assumptions used to apply the Lumped Capacitance Method, the result can be checked using a total energy approach, based the heat transfer rate presented in TABLE IV.

$$q'' A_S t = c_P V_{Tot}\left(T_i - T_f\right)$$

where q'' is the heat transfer rate per unit area. The resulting calculation, which can be found in Appendix D gives $T_f = 59.98\ ℃$, on a total energy basis. The results show that the volume of high temperature water is so high and the heat transfer rate is so low that the heat cannot conduct out of the thermal water quickly enough to have a significant effect over the course of six months. However, since a considerable number of assumptions were made to achieve the

simplicity of the preceding calculations, it will be assumed that, for design purposes, the aquifer temperature at the end of the six month storage period is $T_f = 50$ ℃ .

With the temperature of the water now estimated, it is necessary to determine, to within a reasonable approximation, the temperature of the aquifer at some distance from the thermal front. Since the temperature of the aquifer is not expected to change appreciably in the six month storage period, it will be assumed that the surface temperature of the thermal front does not change significantly with time. Thus, since the aquifer is much larger than the region of thermal storage, the transient heat transfer process will be modeled based on Semi Infinite Solid Method outlined in [3] under the assumption of constant surface temperature. The equation defining this process is as follows [3]:

$$\frac{T(x,t) - T_S}{T_i - T_S} = erf\left(\frac{x}{2\sqrt{\alpha t}}\right)$$

where x is the distance from the thermal front, erf is the error function and α is defined by [3]:

$$\alpha = \frac{k}{\rho c_P}$$

The values for the error function can be found in Appendix E. Since the radius of the thermal reservoir is 39.55 (m), the well separation must be larger than that. Therefore, select a well separation of 50 (m) to begin with, and use the difference of 11 (m) to check what the temperature will be after six months of storage. The results of this calculation can be found in Appendix D, where the result was found to be $(11\ m, 6\ months) = 9.19$ ℃ . Since this is a temperature increase of 0.89 ℃ , a well separation of 50 (m) is deemed acceptable in order to balance the need to minimize system space requirements against the need to minimize the thermal interference between wells.

D. System Design Results

TABLE VII: RESULTS OF THERMAL STORAGE SYSTEM DESIGN

Property	Result	Metric
Aquifer Selected	Lower Carbonate Aquifer	
Borehole Depth	~ 120	m
Borehole Diameter	20 - 22	cm
Well Separation	50	m
Input temperature (Summer)	60	°C
Output Temperature (Winter)	50	°C
Water Volume Stored	24572.16	m^3
Water Flow Rate	5.678	$\frac{m^3}{hr}$
Estimated Heat Recovery Percentage	~ 83.33	%

VII. Environmental and Regulatory Considerations

A. Applicable Codes, Standards and Regulations

Before a system such as that proposed in this paper could be installed on a residential property, there are a number of standards, codes and regulations to be taken into consideration. These standards and codes apply to this project because the system requires not only the use of environmental resources, such as ground water and water wells, but also the handling of regulated chemicals such as the working fluid.

Regulations related to ground water and water wells can be found in The Ground Water and Water Well Act, C.C.S.M. c. G110 [19] and groundwater usage regulations can be found in The Water Right Act [15] . In the province of Manitoba, a license is required to drill, and an applicant

must be in the business of well drilling and be able to demonstrate experience in such a business over a period of time in order for the license to be granted. Furthermore, any person drilling a well, or an owner who wishes to use ground water must take precautions to prevent any pollution or contamination ground water in the area. In Manitoba a license is required for groundwater usage over 25,000 $\left(\frac{L}{day}\right)$ or groundwater usage for irrigation or industrial purposes, including groundwater heating and cooling systems. The Province regulates the right to drill wells primarily for the purpose of preventing ground water contamination. Thus, there are considerable regulatory barriers involved in drilling down to, and withdrawing water from, the aquifer.

The selected working fluid, R134a, also has standards and regulations associated with its use. R-134a, which is a fluorinated ethane compound, has similar physical characteristics as propane, which has lower boiling point and similar heat capacity at constant volume. R-134 is not easily biodegradable and thus leakage into ground water or lakes should be prevented, as the compound will not breakdown naturally [20]. The primary reason R-134a was selected as a working fluid rather than propane, as suggested by the client, or ammonia, is based on safety considerations. Since the system is designed to be installed in a household, it was decided that the risk of explosion or fire with propane, and the higher level of toxicity associated with ammonia outweighed the potential benefits of their use [21]. According to the American Society of Heating , Refrigerting and Air-Conditioning Engineers (ASHRAE) Standard 34, and with reference to Figure 28, R-134 is classified as a member of group A1, or it is not flammable in air, and is not considered to be highly toxic to humans, although its greenhouse gas potential is significantly higher than that of ammonia or propane [22].

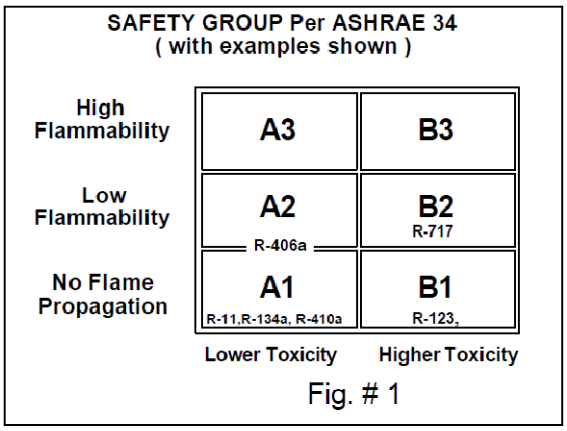

Figure 28: ASHRAE Table of Refrigerant Hazard Rankings [19]

B. Chemical Reactions During Thermal Storage

Because the Geoclimatic system uses groundwater to store thermal energy, chemical reaction occurring in the water and rock strata must be taken into consideration. Thermal energy often acts to accelerate chemical reactions, and the groundwater temperature, when being injected into the aquifer, is approximately 60°C.

It is possible for the heat exchangers, pipes, and aquifer rock could be clogged by Calcite precipitation, since the aquifer is formed largely of limestone [24]. Most of the chemical reactions forming these precipitates are caused by the heating and cooling processes. If groundwater temperature is increased, both the alkalinity and Ca^{+} concentrations are reduced, leading to the formation of calcite precipitates. The process is reversed under cooling, where alkalinity and Ca^{+}concentration increase because of calcite redissolution. The most reactive minerals in groundwater are calcium carbonate, silicate and sulphides. Thus during the design process, and during installation of a system using water wells, knowledge of local groundwater mineral content is important to reduce the risk of clogging pipes or heat exchangers. There are three effective solutions to prevent precipitation of calcite. First, the heated water must be acidified before a heating cycle, thereby increasing decreasing the pH to compensate for the increased alkalinity. The second method involves exchanging Ca^{2+} by $2Na^{+}$ using cation

exchange. The final method, which is recommended as the most efficient method, involves de-carbonation of the water, which means that HCO_3^- ions are replaced by acidic ions such as Cl^{1-} [24]. The CO_2 enters the system by means of $O_2$from the air being dissolved in the water [23]. This can be achieved through the addition of HCL into the water stream, followed by degassing of the CO_2. Another option is to attempt to prevent oxygen from entering the water by capping the boreholes and using elaborate containment to ensure no air can pass [23].

VIII. Economic Analysis

An economic analysis is conducted in Appendix B.

IX. Recommendation for Future Work

Although this report provides a good starting point for the development of Geoclimatic energy, there are still a number of issues that must be addressed before a Geoclimatic energy system can be successfully implemented.

One major shortfall of this report is the analysis of the modified heat pump cycle. The phase transformations during heat transfer causes analytical methods to either be too complicated to solve, or over simplified, as is the case with the analysis presented in this report. As such, the implementation of a computational fluid dynamics (CFD) model would drastically improve the calculation of phase transformations and heat transfer.

Another item which requires major consideration is the “thermo-compression” process by which the super-heated R134a vapour gets isothermally compressed. Although theoretically possible, the implementation of this process is very challenging. This thermo-compression process is essential for the modified heat pump cycle to generate net power, and as such requires significantly more detailed analysis to ensure success of the cycle.

From the perspective of the thermal energy cycle, it is desirable to pursue a larger scale operation which employs the concept of Geoclimatic energy. The temperature differences in the cycle are very low, resulting in the system requiring a very high efficiency. A larger scale operation has the benefits of the economies of scale to help absorb the cost of the high efficiency equipment required as well as to ensure adequate maintenance procedures to prevent decaying system efficiency Geoclimatic energy for use in a commercial setting or for residential heating is worthy of further consideration.

As far as the aquifer thermal storage system is concerned, the data used in this investigation should be subject to scrutiny. It was often selected for regions in the vicinity of the city of Winnipeg, and, even if it originated from a test well within the city, there is such a variation in the properties from one point to the next, the only way to determine the properties with any accuracy would be drill a test well in the intended location and measure them. It is therefore recommended that such measurements should be made before any system is installed.

It is also recommended that the analysis be performed numerically using a commercially available software package, such as FEFLOW. There were a number of assumptions made during the course of this project that, while justified, may give incorrect results. Thus, the analysis should be confirmed by numerical modeling before proceeding further with the design.

X. Conclusions

This project is motivated by the growing demand for alternative sources of energy, as issues such as the trend of increasing energy consumption, the prospect of peak oil, and global warming become more urgent. Many alternative energy sources are already being harnessed, including wind, solar and hydro power. One possible source of energy that is yet to be investigated is the drastic temperature difference that is experienced in certain extreme continental climates, such as Winnipeg.

The concept of Geoclimatic energy is intended as an improvement to conventional geothermal heat pumps by not only providing a home's heating and cooling requirements, but to also generate surplus electricity from seasonal temperature variations. A modified heat pump cycle has been designed which can serve the function of a geothermal heat pump, while simultaneously generating a small surplus of electricity. The ability for thermal energy storage has been investigated with very promising results.

Geoclimatic energy possesses considerable potential to decrease energy consumption related to heating and cooling residential and commercial spaces as well as serve as a supplement to the electrical grid. Although there are a lot of promising signs, there are also a considerable number of challenges that lay on the road ahead. Creative and innovative solutions must be sought to ensure that Geoclimatic energy can one day serve an important role in the emerging world of alternative energy.

XI. References

[1] "Enthalpy," in Wikipedia, the Free Encyclopedia [Online], Nov 26, 2010. Available: http://en.wikipedia.org/wiki/Enthalpy [Dec 4, 2010].

[2] China Harbin Dawn Happy Heat Pipe Technology Co., Ltd. (2008, Apr 24). "826639110.gif," in *The Vapor-Compression Refrigeration Cycle* [Online]. Available: http://china-heatpipe.net/heatpipe04/08/2008-4-24/The_Vapor-Compression_Refrigeration_Cycle.htm [Nov 30, 2010].

[3] F. P. Incropera, D. P. DeWitt, T. L. Bergman and A. S. Lavine, *Fundamentals of Heat and Mass Transfer*, 6th ed. Hoboken, NJ: John Wiley & Sons, Inc., 2007.

[4] R. W. Fox, A. T. McDonald and P. J. Pritchard, *Introduction to Fluid Mechanics*, 6th ed. Hoboken, NJ: John Wiley & Sons, Inc., 2006.

[5] G. Leverick and D. Olmstead, "Design Project: Flat Plate Solar Collector," MECH 3460, Department of Mechanical and Manufacturing Engineering, University of Manitoba, Winnipeg, MB, Apr 1, 2009

[6] DuPont. (2004, Oct). *Thermodynamic Properties of HFC-134a*. Available: http://www2.dupont.com/Refrigerants/en_US/assets/downloads/h47752_hfc134a_thermo_prop_si.pdf [Nov 20, 2010].

[7] Bock Kältemaschinen GmbH. "Bock Compressors: Open type compressor: F3" [Online]. Available: http://www.bock.de/ArticlePrint.aspx?ArticleID=1167&lang=en&TabIndex=1&RefrigerantID=15 [Nov 27, 2010].

[8] S. Earle. (2006). *GEOL-304 – Hydrogeology – Properties of aquifers* [Online]. Available: http://web.viu.ca/earle/geol304/geol-304-b.pdf [Nov 5, 2010].

[9] The International Development Research Centre. [Feb 21, 2005). *Chapter 5. Groundwater sources* [Online]. Available: http://www.idrc.ca/en/ev-29702-201-1-DO_TOPIC.html [Nov 5, 2010].

[10] Argonne National Laboratory Environmental Science Division. *Hydraulic Conductivity* [Online]. Available: http://web.ead.anl.gov/resrad/datacoll/conuct.htm [Nov 27, 2010].

[11] F.J. Molz, J.C. Warman and T.E. Jones. (July 1978). "Aquifer Storage of Heated Water: Part I – A Field Experiment," *Ground Water* [Online], vol. 16 (4), pp. 234 - 241. Available: http://info.ngwa.org/gwol/pdf/782000871.PDF [Nov 5, 2010].

[12] G. A. Ferguson, R.N. Betcher, S.E. Grasby. (Nov 2006). "Hydrogeology of the Winnipeg Formation in Manitoba, Canada," *Hydrogeology Journal* [Online], vol. 15 (3), pp. 573-587. Available: SpringerLink [Nov 5, 2010].

[13] G.A.G. Ferguson, "Groundwater and Heat Flow in Southeastern Manitoba: Implications to Water Supply and Thermal Energy," Ph. D. dissertation, Dept. Civl. Eng., Univ. of MB, Winnipeg, MB, 2004. Available: http://mspace.lib.umanitoba.ca/bitstream/1993/3799/1/Ferguson,%20Groundwater%20and.pdf [Nov 5, 2010].

[14] G. Ferguson, S. St. George. (Oct 2003). "Historical and Estimated Ground Water Levels Near Winnipeg, Canada, and Their Sensitivity to Climatic Variability," *Journal of the American Water Resources Association* [Online], vol. 39 (5), pp. 1294-1259. Available: http://people.stfx.ca/gferguso/Ferguson%20and%20St.%20George.pdf [Nov 5, 2010].

[15] R. Betcher, G. Grove, and C. Pupp (1995, March). "*Groundwater In Manitoba: Hydrogeology, Quality Concerns, Management*" [Online]. Available: http://www.thinktrees.org/my_folders/Envirothon_Theme_Resources_2010/hg_of_manitoba.pdf [Nov 5, 2010].

[16] Z. Şen (1996). "A Graphical Method for Storage Coefficient Determination from Quasi-Steady State Flow Data," *Nordic Hydrology* [Online], vol. 27 (4), pp. 247 – 254. Available: http://www.iwaponline.com/nh/027/0247/0270247.pdf [Nov. 27, 2010].

[17] Geo-Slope International. *Temp/W 2007* [CD-ROM]. Calgary, AB: 2007.

[18] G. Ferguson, A.D. Woodbury and G.L.D. Matile. (Sept 2003). "Estimating Deep Recharge Rates Beneath an Interbolate Moraine Using Temperature Logs," *Ground Water* [Online], vol. 41 (5), pp. 640 - 646. Available: http://info.ngwa.org/gwol/pdf/782000871.PDF [Nov 5, 2010].

[19] Canadian Legal Information Institute. (2010, Oct. 22). "*Ground Water and Water Well Act, C.C.C.M. c. G110*" [Online]. Available: http://www.canlii.org/en/mb/laws/stat/ccsm-c-g110/latest/ccsm-c-g110.html#history [Oct 27, 2010].

[20] W. Goetzler, J. Burgos, H. Hiraiwa, and T. Sutherland. (2010, April). *Review of regulations and standards for the use of refrigerants with GWP values less than 20 in HVAC&R Applications.* NAVIGANT Consulting, INC. Burlington, USA. Available: http://www.ahrinet.org/Content/downloads/research/Research-Final/ARTI-Rpt-09001-01.pdf [Oct 27, 2010].

[21] GEA GRASSO. "*Safety Instructions Refrigerant R134A*" [Online]. Available: http://docnav.grasso-global.com/DocNav_Eng/Sources_e/Ber_e/_724011_si_km_r134a_gbr_1_.pdf [Oct 27, 2010].

[22] J. Parsnow. *Three Important Questions to answer on Alternative Refrigerants.* Environmental System Marketing Carrier Corporation. USA. Available: http://www.xpedio.carrier.com/idc/groups/public/documents/marketing/wp020.pdf [Oct 27, 2010].

[23] P. Seibt. (Sept 2003). "Reinjection of thermal waters into sandstone reservoirs in the North German Basin," in *International Geothermal Conference* [Online], Reykjavik, Iceland, 2003, pp. 15 – 20. Available: http://www.jardhitafelag.is/media/PDF/S09Paper064.pdf [Nov 5, 2010].

[24] A. Willemsen and C.A.J. Appelo, "*Chemical Reactions During Heat Storage in Shallow Aquifers In The Netherlands: Laboratory Experiments And Geochemical Modelling*"[Online], Hydrogeology in the Service of Man, Memories of the 18th Congress of the International Association of Hydrogeologists, Cambridge, 1985. Available: http://iahs.info/redbooks/a154/iahs_154_04_0068.pdf [Nov 15, 2010].

[25] Coolgas. *R-134a Products* [Online]. Available: http://www.r-134a.com/ [Oct 20, 2010].

[26] Charlotte Pipe and Foundry Company. (Oct, 2010). *Plastic Pipe for Drainage & Pressure Applications* [Online]. Available: http://www.charlottepipe.com/Products/Assets/02C-PVC_List_Price/LP-PPDP%20(1010).pdf. [Oct 25, 2010].

[27] Alibaba. (2010). *MS Series Hydraulic Motor* [Online]. Available: http://hydraulic-china.en.alibaba.com/product/347226376200199117/MS_Series_Hydraulic_motor.html [Nov 16, 2010].

[28] Base cost estimation of heat exchanger designs; Power point presentation wps.prenhall.com/wps/media/objects/148/.../heat_exchanger.ppt

[29] http://www.globalspec.com/SpecSearch/PartSpecs?partId={5F86736D-FA5D-4358-A19D-0958E6FCC11B}&vid=102151&comp=1594&qid=19390178

XII. Appendices

A. Conceptual Selection

After having considered the project objectives and generated a number of design concepts, it was necessary to find a method of comparing the various options in order to screen the various options. Due to the complexity of the proposed system, it was decided to develop concepts for the individual components of the system, rather than consider redesigning the client's concept.

1. Working Fluid

For the purposes of this project, the working fluid is the fluid which will act as the thermal energy carrier between two points in the system. As a result, the properties of the prospective fluids are of prime importance to the effective operation of the system as a whole.

Three popular refrigerants, propane, R134a and ammonia, were selected for comparison. As the basis for comparison, several properties were compared, including specific heat, thermal conductivity, dynamic viscosity, environmental impact and safety considerations. While there were minor variations in the heat transfer properties of the various fluids, it was decided that the environmental and safety considerations were of greater importance. Furthermore, when the various ecological and health issues were taken into consideration, R134a was selected as the working fluid for this system, as it was decided that propane carries an unacceptably high risk of explosion and ammonia is too toxic to be installed into a home.

2. Power Extraction

The objective of this system is to extract useable power from the operation of the system. Therefore, it was necessary to select a mechanical method for converting the thermal energy carried by the working fluid in mechanical shaft power. Three possible options were originally selected which included a vane motor, a gear motor, or a kinetic turbine. Later in the project, a

turbo-expander, a turbomachine which converts pressure into shaft power by expanding potentially low temperature fluids, was added as an option. It was possible to reject the kinetic turbine initially due the complexities and costs associated with such a machine for a small scale project. However, the kinetic turbine remains a viable, and in fact appealing, option for potential larger scale projects in the future.

It was eventually decided to select the turbo-expander as the most suitable expansion device, despite the difficulties locating one of suitable size. Gear motors and gear pumps were, based on initial studies of their capabilities, unable to meet the needs of the modified refrigeration cycle. As the cycle was being designed, there was strong possibility that a phase change would occur during the expansion process. Since gear and vane motors are not generally designed to operate in multi-phase flow, they would not be suitable for such a cycle.

3. Heat Collection

Geoclimatic energy relies on the temperature difference between the ground and the ambient air to generate power. Three possible methods of exchanging heat between the working fluid and the ambient air have been devised; natural convection, an asphalt driveway heat collector, and a solar collector. Utilizing natural convection is, by far, the simplest means of exchanging heat between the working fluid and the ambient air. In this method, the ambient air is allowed to interact with the pipes containing the working fluid. This method has the advantage of being very cheap to build. However, if the input temperature is limited to that of the ambient air, longer pipes may be required to optimize the maximum temperature of the working fluid. Thus, the thermal efficiency of this concept may be limited because increasing the length of the piping will result in a larger pressure drop in the line.

The second option involves collecting solar energy in the summer, which would lead to a larger temperature difference in the power generation cycle. One means of collecting solar energy would be to embed the pipes in an asphalt driveway. The sun's energy would heat the asphalt,

causing the asphalt's temperature to exceed ambient. The disadvantage of this idea is that in the winter, the solar collector would reduce the temperature difference, as the temperature of the asphalt would depend primarily on the solar incidence, and therefore, would be at a higher temperature than the ambient. Even if this problem were resolved by covering the driveway with snow, it would be insulated from the ambient, and thus still warming, meaning some form of bypass would be required.

Another option for collecting solar energy is to utilize a commercially available solar collector, which would enable even higher temperatures to be achieved during the summer. This method of solar collection shares the disadvantage of the asphalt driveway solar collection system. Thus, since the collector would be counter-productive in the winter, the system would have to be bypassed. The higher temperature achievable by a commercial solar collector is countered by its higher cost, and more involved maintenance requirements.

4. Heat Storage

The other thermal cornerstone of a Geoclimatic Energy system is storing collected heat energy in the ground. Maximizing heat storage increases the potential temperature difference of the cycle, and therefore its Carnot efficiency. Two methods of storing heat between summer and winter were investigated; using the aquifer and using a close-loop refrigerant cycle.

The aquifer system relies on pumping water from one place in the aquifer to another and using the earth's constant temperature to provide a stable environment to reduce heat transfer losses. In this case, the loop is open, with water being able to flow independently of the loop. The closed loop system operates by installing loops of piping in the ground to act as heat exchanger, and then uses the earth as a heat sink.

It was decided to select the aquifer storage method, as recommended by the client. The closed loop system is more difficult to install and, due to the relatively shallow depth, doesn't have the

same degree of thermal stability as the aquifer system, which has deep boreholes. Furthermore, the heat capacity of the ground is much lower than that of water, meaning that more ground volume would be required to store the needed heat. Also, preliminary studies of aquifer properties indicated that the aquifer had low flow rates and a sufficient quantity of water, as well as desirable thermal properties to meet the needs of the system being proposed.

B. Economic Analysis

Before the system is installed and proper operation commences, it is imperative that an economic analysis be carried out over the course of an estimated twenty-five year lifetime. The analysis will allow for a determination of the break-even point, if it exists, of future costs, revenue, annual savings and income as well as rate of return on capital investments by projecting current costs. The costs will be projected using a host of economic factors and governmental variables such as economic inflation rate, incentives, grants and governmental loans. Thus, the financial viability of the project can be determined

1. Equipment Costs

In coming up with the cost of the equipment, it was decided to keep cost down by utilizing off the shelf components that where readily available. By keeping the design of new parts to a minimum, considerable time and money will be saved, as well as any maintenance and repair issues that may arise in the future. Due to the wide scope of this project, as well as the number of changing parameters, the project requires a considerable amount of equipment that would be working simultaneously to meet the final requirement of power generation. It is necessary therefore to minimize the amount of money that would be spent in both purchasing and designing the necessary parts. Bearing this in mind, various suppliers of the equipment and services that would be needed for this project were contacted. The costs can be broken down into working fluid costs, piping costs, equipment costs and drilling costs.

a) Working Fluid Cost

The selected working fluid was R-134a, which was chosen based on the disadvantages of ammonia and propane as described above. Other factors include cost of the fluid, the relative availability, efficiency of the fluid, acceptable ISO standards and codes with respect to toxicity to the environment as well as the Global Warming Potential [GWP].

The cost per metric ton of R-134a is calculated as:

$$\$8/0.3396kg \text{ X } (1000kG) = \$23,557 \quad [25]$$

Thus a minimum of roughly $23,600 would be needed to purchase a metric ton of R-134a. The cost available in the market is treated via dollar per metric ton, but for this project, which is residential in nature, this amount of working fluid would be excessive and the required ISO standard states that an individual can only have 3 Kg of gas in their home [20]. Therefore to get the cost per 3 Kg of gas, divide the value by 333, since 333 by 3 is roughly a ton. This gives a value of roughly 70$ per 3 kg of working fluid.

b) Piping Cost

TABLE VIII: PVC PIPING COST COMPARISON [26]

PVC Pipes Size	Price per Foot
½”	$0.42
¾”	$0.54
1”	$0.80
1 ½”	$1.24
2”	$1.62
4”	$4.60
6”	$8.16

TABLE VIII shows the cost per foot of pipe for different diameters. It was decided to use 1-inch diameter piping, which would yield a suitable flow, with a cost of $0.80 dollar per foot. Therefore for a 400 foot piping, a total cost of $292 would be needed.

c) Equipment and Drilling

TABLE IX: APPROXIMATE COSTS OF MECHANICAL COMPONENTS

Equipment	**Cost**
Air Motor	$150 per 1500 set [27]
Heat Exchanger i. Shell and tube or ii. Counter Flow or iii. Cross Flow	 $14,400 $63,400 $2200 [28]
Compressor	$2,500 (quote Dekker Vacuum Tech.) [29]
Solar Collector	About $1200 to build
Ball Valves (x12)	345 x 12 = $4140 (Quote from keywin Ind Ltd.
Bore hole drilling	$30 per foot = 30 x 2(130) = $7800
Approximate Total	$17,800

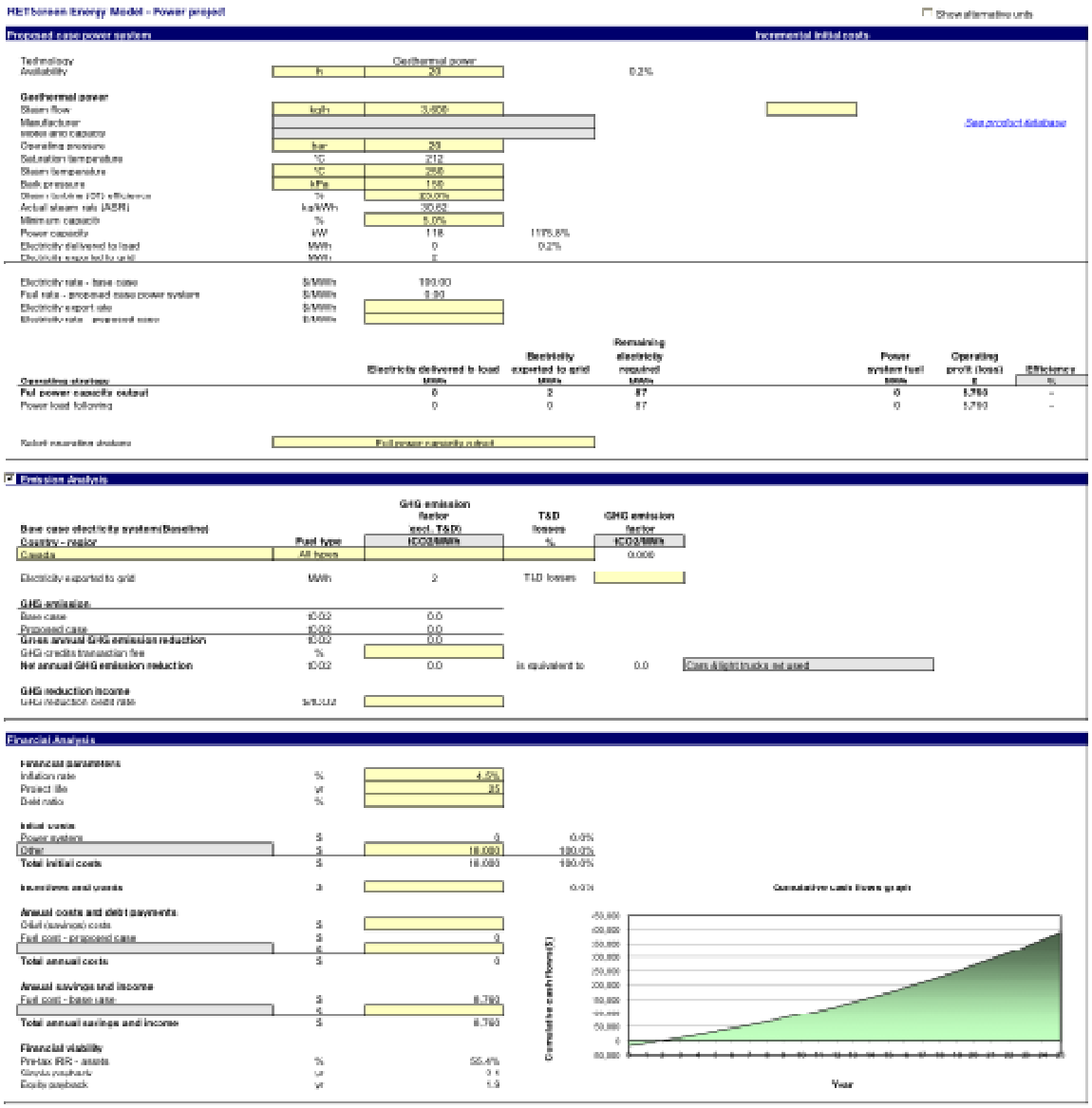

Figure 29: Economic projections showing break-even point

The above analysis shows that a break-even point would be reached in about 2 to 3 years on an initial capital cost of approximately $18 000. The analysis also has tabs for governmental grants and incentives, which were left blank in the absence of additional information. This analysis considers the worst case scenario in which the entire capital cost would have to be paid by the client. A total life cycle of 25 years has been used.

C. Thermal Energy Cycle Calculations

1. Summer Cycle Sample Calculation

Initial State												
T_2	70	[C]										
P_2	1800	[kPa]										
h_2	437.4	[kJ/kg]										
s_2	1.7306	[kJ/ kg K]										
v_2	0.01134	[m^3 / kg]										
m_dot	1.7	[kg/s]										
Compressor												
S_r_i	1.7306	[kJ/kg K]										
η	0.99											
S_r_o	1.74808081	[kJ/kg K]										
T_3	96.7	[C]										
P_3	2800	[kPa]										
h_3	452.7	[kJ/kg]										
v_3	0.00722	[m^3 / kg]										
m_dot	1.7	[kg/s]										
W	26.01	[kW]										
Cold Well Heat Exchanger												
Water Properties			**R134a Properties**			**Water Pipe Properties**			**Refrigerant Pipe Properties**			
k	0.59	[W/mK]	k	0.0531	[W/mK]	D	0.08	[m]	D	0.03	[m]	
μ	0.001225	[Ns/m2]	μ	6.68E-05	[Ns/m2]	L	25	[m]	L	25	[m]	
ρ	1000	[kg/m3]	ρ	823.4	[kg/m3]	t	0.002	[m]	t	0.002	[m]	
v	1.225E-06	[m2/s]	v	8.11E-08	[m2/s]	A	0.0043197	[m2]	A	0.00070686	[m2]	
Cp	4.189	[kJ/kgK]	Cp	3.001	[kJ/kgK]	P	0.2513274	[m]	P	0.09424778	[m]	
Pr	7.56		Pr	3.775269					k	401	[W/mK]	
m_dot	1	[kg/s]	m_dot	1.7	[kg/s]							
Q	0.001	[m3/s]	Q	0.002065	[m3/s]							
T_i	10	[C]	T_i	96.7	[C]							
Re	15118.2432		Re	1080093								
f	0.0281265		f	0.011475								
Nu	119.211351		Nu	3467.465					**Pressure Losses**			
h	879.183717		h	6137.414					Elbows	4	[#]	
									L_e/D	30	[unitless]	
									h_l_minor	5.87384784	[m^2/s^2]	
C_min	4189								h_l_major	81.5812201	[m^2/s^2]	
UA	3961.18914								h_l_total	87.4550679	[m^2/s^2]	
NTU	0.94561689								ΔP	7.34052017	[kPa]	
Cr	0.2											
ε	0.58566215											
q	212.70447	kW							Δh required	124.2	[kJ/kg]	
									Δh actual	125.120276	[kJ/kg]	
T_w_o	60.7769085	[C]										
T_4	82.9	[C]										
P_4	2792.65948	[kPa]										
h_4	328.5	[kJ/kg]										
s_4	1.4005	[kJ/kg K]										
v_4	0.0011	[m^3 / kg]										
m_dot	1.7	[kg/s]										

Turbo-Expander

S_r_i	1.4005	[kJ/kg K]
η	0.98	
S_r_o	1.42908163	[kJ/kg K]
T_5	-15	[C]
P_5	163.9	[kPa]
h_5	310.2	[kJ/kg]
x_5	0.62	[unitless]
v_5	0.0751	[m^3 / kg]
m_dot	1.7	[kg/s]
W	31.11	[kW]

Air Conditioning

Air Properties

k	0.0263	[W/mK]
μ	1.85E-05	[Ns/m2]
ρ	1.1614	[kg/m3]
v	1.5895E-05	[m2/s]
Cp	3.01E-03	[kJ/kgK]
Pr	0.707	
m_dot	0.1	[kg/s]
Q	0.08610298	[m3/s]
T_i	30	[C]
Re	18491.3914	
f	0.02668345	
Nu	48.6051166	
h	3.19578642	
C_min	0.30	
UA	7.94	
NTU	26.40	
Cr	0.00	
ε	1.00	
q	13.53	kW
T_a_o	-15.00	[C]
T_5	-15	[C]
P_5	160.574593	[kPa]
h_5	318.159706	[kJ/kg]
v_5	0.0751	[m^3 / kg]
m_dot	1.7	[kg/s]

R134a Properties

k	0.0718	[W/mK]
μ	0.000148	[Ns/m2]
ρ	13.31558	[kg/m3]
v	1.11E-05	[m2/s]
Cp	1.481	[kJ/kgK]
Pr	3.048632	
m_dot	1.7	[kg/s]
Q	0.12767	[m3/s]
T_i	-15	[C]
Re	488161.3	
f	0.013188	
Nu	1560.92	
h	3735.801	

Air Duct Properties

D_eq	0.4	[m]
L	2	[m]
t	0.002	[m]
A	0.1171814	[m2]
P	1.2566371	[m]

Refrigerant Pipe Properties

D	0.03	[m]
L	2	[m]
t	0.002	[m]
A	0.0084823	[m2]
P	0.09424778	[m]
n	12	[#]
k	401	[W/mK]

Pressure Losses

Elbows	28	[#]
L_e/D	30	[unitless]
h_l_minor	1254.84225	[m^2/s^2]
h_l_major	1195.08786	[m^2/s^2]
h_l_total	2449.93011	[m^2/s^2]
ΔP	3.32540658	[kPa]
Δh actual	7.95970588	[kJ/kg]

Solar Collector

R134a Properties			Refrigerant Pipe Properties			Solar Collector Properties					
k	0.0718	[W/mK]	D	0.03	[m]	U_c	15	[W/m^2 K]			
μ	0.0001478	[Ns/m2]	L	2	[m]	q_rad	800	[W/m^2]			
ρ	13.3155792	[kg/m3]	t	0.002	[m]	w_c	5	[m]			
v	1.11E-05	[m2/s]	A	0.003534	[m2]	L	2	[m]			
Cp	1.481	[kJ/kgK]	P	0.094248	[m]	A_c	10	[m^2]			
Pr	3.04863231		n	5	[#]	T_amb	30	[C]			
m_dot	1.7	[kg/s]	k	401	[W/mK]	T_eq	83.333333				
Q	0.12767	[m3/s]									
T_i	-15	[C]									
Re	1171587.13										
f	0.01131889										
Nu	3307.24256										
h	7915.33386								**Pressure Losses**		
									Elbows	12	[#]
									L_e/D	30	[unitless]
C_min	2517.70								h_l_minor	2658.57625	[m^2/s^2]
UA	6155.90								h_l_major	2461.64467	[m^2/s^2]
NTU	2.45E+00								h_l_total	5120.22092	[m^2/s^2]
Cr	0.00								ΔP	6.9499192	[kPa]
ε	0.9133										
q	226.10	kW									
T_2	70	[C]									
P_2	1800	[kPa]									
h_2	437.4	[kJ/kg]									
s_2	1.7306	[kJ/ kg K]									
v_2	0.01134	[m^3 / kg]									
m_dot	1.7	[kg/s]									

2. Winter Cycle Sample Calculation

Initial State		
T_2	50	[C]
P_2	1300	[kPa]
h_2	424.3	[kJ/kg]
s_2	1.711	[kJ/ kg K]
v_2	0.01542	[m^3 / kg]
m_dot	1.4	[kg/s]

Compressor		
S_r_i	1.711	[kJ/kg K]
η	0.99	
S_r_o	1.728283	[kJ/kg K]
T_3	92	[C]
P_3	2800	[kPa]
h_3	445.4	[kJ/kg]
v_3	0.00684	[m^3 / kg]
m_dot	1.4	[kg/s]
W	29.54	[kW]

Air Heating

Air Properties			R134a Properties			Air Duct Properties			Refrigerant Pipe Properties		
k	0.0263	[W/mK]	k	0.0718	[W/mK]	D_eq	0.4	[m]	D	0.03	[m]
μ	1.85E-05	[Ns/m2]	μ	0.000148	[Ns/m2]	L	2	[m]	L	2	[m]
ρ	1.1614	[kg/m3]	ρ	146.1988	[kg/m3]	t	0.002	[m]	t	0.002	[m]
v	1.59E-05	[m2/s]	v	1.01E-06	[m2/s]	A	0.117181	[m2]	A	0.008482	[m2]
Cp	3.01E-03	[kJ/kgK]	Cp	1.481	[kJ/kgK]	P	1.256637	[m]	P	0.094248	[m]
Pr	0.707		Pr	3.048632					n	12	[#]
m_dot	0.1	[kg/s]	m_dot	1.4	[kg/s]				k	401	[W/mK]
Q	0.086103	[m3/s]	Q	0.009576	[m3/s]						
T_i	-20	[C]	T_i	92	[C]						
Re	18491.39		Re	402015.2							
f	0.026683		f	0.013666							
Nu	48.60512		Nu	1322.791							
h	3.195786		h	3165.881					**Pressure Losses**		
									Elbows	28	[#]
									L_e/D	30	[unitless]
C_min	0.30								h_l_minor	7.315026	[m^2/s^2]
UA	7.92								h_l_major	6.966692	[m^2/s^2]
NTU	26.35								h_l_total	14.28172	[m^2/s^2]
Cr	0.00								ΔP	0.212841	[kPa]
ε	1.00										
q	-33.68	kW									
T_a_o	92.00	[C]							Δh actual	-24.056	[kJ/kg]
T_4	82.8	[C]									
P_4	2799.787	[kPa]									
h_4	421.344	[kJ/kg]									
v_4	0.0011	[m^3 / kg]									
m_dot	1.4	[kg/s]									

Water Heater

Water Properties			R134a Properties			Refrigerant Pipe Properties					
k	0.59	[W/mK]	k	0.0718	[W/mK]	D	0.03	[m]			
μ	0.001225	[Ns/m2]	μ	0.000148	[Ns/m2]	L	2	[m]			
ρ	1000	[kg/m3]	ρ	909.0909	[kg/m3]	t	0.001	[m]			
v	1.23E-06	[m2/s]	v	1.63E-07	[m2/s]	A	0.000707	[m2]			
Cp	4.189	[kJ/kgK]	Cp	1.481	[kJ/kgK]	P	0.094248	[m]			
Pr	7.56		Pr	3.048632		n	34	[# of loops]			
α	2.25E-05	[m2/s]	m_dot	1.4	[kg/s]	k	401	[W/mK]			
			Q	0.00154	[m3/s]						
T_amb	5	[C]	T_i	82.8	[C]						
β	-0.01997		Re	402015.2							
Ra	4.42E+12		f	0.013666							
Nu	2268.981		Nu	1322.791							
h	669.3493		h	3165.881					**Pressure Losses**		
									Elbows	72	[#]
									L_e/D	30	[unitless]
C_min	2073.4								h_l_minor	70.05288	[m^2/s^2]
UA	3377.34								h_l_major	73.51228	[m^2/s^2]
NTU	1.62889								h_l_total	143.5652	[m^2/s^2]
Cr	0								ΔP	13.30416	[kPa]
ε	0.803853										
q	-129.67	kW									
									Δh required	-92.944	[kJ/kg]
T_4	82.8	[C]							Δh actual	-92.6214	[kJ/kg]
P_4	2786.48	[kPa]									
h_4	328.7226	[kJ/kg]									
s_4	1.40001	[kJ/kg K]									
v_4	0.0011	[m^3 / kg]									
m_dot	1.4	[kg/s]									

Turbo-Expander

S_r_i	1.40001	[kJ/kg K]									
η	0.98										
S_r_o	1.428582	[kJ/kg K]									
T_5	-30	[C]									
P_5	84.29	[kPa]									
h_5	301.9	[kJ/kg]									
x_5	0.642	[unitless]									
m_dot	1.4	[kg/s]									
W	37.5517	[kW]									

Hot Well Heat Exchanger											
Water Properties			**R134a Properties**			**Water Pipe Properties**			**Refrigerant Pipe Properties**		
k	0.59	[W/mK]	k	0.0531	[W/mK]	D	0.08	[m]	D	0.03	[m]
μ	0.001225	[Ns/m2]	μ	6.68E-05	[Ns/m2]	L	25	[m]	L	40	[m]
ρ	1000	[kg/m3]	ρ	823.4	[kg/m3]	t	0.002	[m]	t	0.002	[m]
v	1.23E-06	[m2/s]	v	8.11E-08	[m2/s]	A	0.00432	[m2]	A	0.000707	[m2]
Cp	4.189	[kJ/kgK]	Cp	3.001	[kJ/kgK]	P	0.251327	[m]	P	0.094248	[m]
Pr	7.56		Pr	3.775269					k	401	[W/mK]
m_dot	1	[kg/s]	m_dot	1.4	[kg/s]						
Q	0.001	[m3/s]	Q	0.0017	[m3/s]						
T_i	50	[C]	T_i	-30	[C]						
Re	15118.24		Re	889488.7							
f	0.028126		f	0.011862							
Nu	119.2114		Nu	2931.265					**Pressure Losses**		
h	879.1837		h	5188.339					Elbows	4	[#]
									L_e/D	30	[unitless]
									h_l_minor	4.117855	[m^2/s^2]
C_min	4189								h_l_major	91.50789	[m^2/s^2]
UA	4281.343								h_l_total	95.62575	[m^2/s^2]
NTU	1.022044								ΔP	8.026324	[kPa]
Cr	0.2										
ε	0.612617										
q	205.3001	kW							Δh required	145	[kJ/kg]
									Δh actual	146.6429	[kJ/kg]
T_w_o	0.990675	[C]									
T_4	50	[C]									
P_4	76.26368	[kPa]									
h_4	448.5429	[kJ/kg]									
s_4	1.9916	[kJ/kg K]									
v_4	0.3252	[m^3 / kg]									
m_dot	1.4	[kg/s]									

D. Thermal Storage Calculations

1. Lumped Capacitance Calculations

$$\frac{T(t) - T_\infty}{T_i - T_\infty} = exp\left[-\left(\frac{kA_S}{h}\right)\left(\frac{1}{\rho V c_P}\right)t\right]$$

Isolating for the Temperature as a function of time, T(t), gives,

$$T(t) = (T_i - T_\infty)\, exp\left[-\left(\frac{kA_S}{h}\right)\left(\frac{1}{\rho V c_P}\right)t\right] + T_\infty$$

$$T(t) = (60 - 8.3)exp\left[-\left(\frac{(2.4)2\pi(39.55)(25)}{(25)}\right)\left(\frac{t}{(2416.17)(122860.8)(1359.0)}\right)\right] + 8.3$$

However, the temperatures need to be in degrees Kelvin, and the time is the number of seconds in a six month period, found from:

$$t = 6\ \cancel{months} \times \frac{30\ \cancel{days}}{1\ \cancel{month}} \times \frac{24\ \cancel{hr}}{1\ \cancel{day}} \times \frac{60\ \cancel{min}}{1\ \cancel{hr}} \times \frac{60\ s}{1\ \cancel{min}} = 15552000\ (s)$$

When this calculation is performed, the result is:

$$T(6\ months) = 58.82\ ℃$$

2. Heat Capacity and Total Energy Approach

The general equation relating energy and heat transfer is:

$$q'' = c_P Q\left(T_i - T_f\right)$$

where Q is the volumetric flow rate. This equation can be reorganized into:

$$q'' A_S t = c_P V_{Tot}\left(T_i - T_f\right)$$

$$(84 \times 10^{-3})\left(2\pi(39.55)(25)\right)(15552000) = (3284 \times 10^3)(122860.8)\left[333.15 - T_f\right]$$

Solving for T_f gives:

$$T_f(6\ months) = 59.98\ ℃$$

3. Heat Conduction Between Thermal Storage Wells

The equation defining the time varying temperature of a semi-infinite solid under constant surface temperature conditions is:

$$\frac{T(x,t) - T_S}{T_i - T_S} = erf\left(\frac{x}{2\sqrt{\alpha t}}\right)$$

The first step of this calculation is to determine the argument of the error function:

$$\alpha = \frac{11}{2\sqrt{\left(\frac{2.4}{(2416.17)(1359)}\right)(15552000)}} = 1.63$$

Since 1.63 is not a value on the table of error function values, interpolate to find the value of erf:

$$\frac{1.7 - 1.6}{0.98379 - 0.97635} = 13.44 = \frac{1.7 - 1.63}{0.98379 - x}$$

$$x = 0.97858$$

This result leads to:

$$\frac{T(x,t) - 50}{8.3 - 50} = 0.97858$$

Thus,

$$T(11\ m, 6\ months) = 9.19\ ℃$$

E. Tables and Graphs

Table X: TABLE OF VALUES FOR THE ERROR FUNCTION [3]

x	erf(x)	erfc(x)	x	erf(x)	erfc(x)
0.00	0.0000000	1.0000000	1.30	0.9340079	0.0659921
0.05	0.0563720	0.9436280	1.40	0.9522851	0.0477149
0.10	0.1124629	0.8875371	1.50	0.9661051	0.0338949
0.15	0.1679960	0.8320040	1.60	0.9763484	0.0236516
0.20	0.2227026	0.7772974	1.70	0.9837905	0.0162095
0.25	0.2763264	0.7236736	1.80	0.9890905	0.0109095
0.30	0.3286268	0.6713732	1.90	0.9927904	0.0072096
0.35	0.3793821	0.6206179	2.00	0.9953223	0.0046777
0.40	0.4283924	0.5716076	2.10	0.9970205	0.0029795
0.45	0.4754817	0.5245183	2.20	0.9981372	0.0018628
0.50	0.5204999	0.4795001	2.30	0.9988568	0.0011432
0.55	0.5633234	0.4366766	2.40	0.9993115	0.0006885
0.60	0.6038561	0.3961439	2.50	0.9995930	0.0004070
0.65	0.6420293	0.3579707	2.60	0.9997640	0.0002360
0.70	0.6778012	0.3221988	2.70	0.9998657	0.0001343
0.75	0.7111556	0.2888444	2.80	0.9999250	0.0000750
0.80	0.7421010	0.2578990	2.90	0.9999589	0.0000411
0.85	0.7706681	0.2293319	3.00	0.9999779	0.0000221
0.90	0.7969082	0.2030918	3.10	0.9999884	0.0000116
0.95	0.8208908	0.1791092	3.20	0.9999940	0.0000060
1.00	0.8427008	0.1572992	3.30	0.9999969	0.0000031
1.10	0.8802051	0.1197949	3.40	0.9999985	0.0000015
1.20	0.9103140	0.0896860	3.50	0.9999993	0.0000007